

Contents

Contents.....	1
Abbreviations.....	3
Summary.....	6
Zusammenfassung.....	7
1 Introduction.....	8
1.1 Pancreatic ductal adenocarcinoma - pathogenesis, therapy and outcome.....	8
1.2 Epithelial mesenchymal transition and metastatic potential.....	9
1.3 Estrogen and estrogen receptor α in cancerous EMT.....	11
1.4 Metastasis-associated gene/protein 3 in cancerous EMT.....	12
1.5 Hypothesis and question.....	13
2 Material and Methods.....	15
2.1 Material.....	15
2.1.1 Chemicals and Reagents.....	15
2.1.2 Consumable supply.....	17
2.1.3 Equipment.....	18
2.1.4 Primers for RT-PCR.....	19
2.1.5 Antibodies.....	20
2.1.6 Cell culture media.....	21
2.1.7 Solutions.....	22
2.1.8 Clinical data of pancreatic cancer patients.....	26
2.1.9 Cell lines.....	27
2.2 Methods.....	27
2.2.1 Cell culture and preparation of cells for IHC.....	27
2.2.2 Orthotopic nude mouse model for pancreatic cancer.....	28
2.2.3 Immunohistochemistry.....	28
2.2.4 Western blot analysis.....	31
2.2.5 Reverse transcription and polymerase chain reaction.....	34
2.2.6 Statistic analysis.....	36
3 Results.....	37
3.1 Localization of molecules of the ERα signaling pathway and proliferation in primary human PDAC tissues <i>in-situ</i>.....	37
3.1.1 ER α	37
3.1.2 MTA3, Snail and E-cadherin.....	38
3.1.3 Correlation of ER α , MTA3, Snail and E-cadherin in human PDAC.....	41
3.1.4 <i>In-situ</i> proliferation.....	42
3.2 Molecules of the ERα signaling pathway in human pancreatic cancer cell lines <i>in vitro</i>	43
3.2.1 Localization by immunocytochemistry/immunofluorescence.....	43
3.2.2 Expression of ER α , MTA3, Snail, and E-cadherin at mRNA level of pancreatic cancer cell lines.....	50
3.2.3 Overall expression at the protein level.....	51
3.3 Localization of molecules of the ERα signaling pathway and proliferation within orthotopic xenografts of human pancreatic cancer cell lines in nude mice <i>in situ</i>.....	52
3.3.1 ER α	52
3.3.2 MTA3.....	54
3.3.3 Snail.....	56

Contents

3.3.4	E-cadherin.....	58
3.3.5	<i>In-situ</i> proliferation.....	60
4	<i>Discussion</i>	62
4.1	Background	62
4.2	Human tissues	62
4.3	Pancreatic cell lines	64
4.4	Orthotopic xenograft models of pancreatic cells	67
4.5	Conclusion	68
5	<i>References</i>	69
	<i>Curriculum vitae</i>	74
	<i>Affidavit</i>	75
	<i>Acknowledgements</i>	75

Abbreviations

5-FU	5-Fluorouracil
APS	Ammonium peroxydisulfate
β -ME	Beta-Mercaptoethanol
BCA	Bicinchoninic acid
BMP	Bone morphogenetic proteins
Bp	Base pair
BSA	Bovine serum albumin
CD	Cluster of differentiation
cDNA	Complementary deoxyribonucleic acid
COX 2	Cyclooxygenase 2
DAB	3, 3'-diaminobenzidine
DAPI	4',6-diamidino-2-phenylindole
dd water	Double distilled water
DMEM	Dulbecco's modified eagle medium
DMPC	Di-methyl pyrocarbonate
DMSO	Dimethyl sulfoxide
DNA	Deoxyribonucleic acid
dNTP	Deoxynucleotide triphosphates
DSMZ	Deutsche Sammlung von Mikroorganismen und Zellkulturen
ECACC	European Collection of Cell Cultures
ECM	Extracellular matrix
EDTA	Ethylene diamine tetraacetic acid
EGFR	Epidermal growth factor receptor
EMT	Epithelial-mesenchymal transition
ERE	Estrogen-responsive element
ER α	Estrogen receptor α
FCS	Fetal calf serum
FFPE	Formalin-fixed paraffin-embedded
HCL	Hydrochloric acid
HDAC	Histone deacetylase
HGF	Hepatocyte growth factor

Abbreviations

HNSCC	Head and neck squamous cell carcinoma
HPF	High power field
IHC	Immunohistochemistry
IRS	Immunohistochemical reaction score
kDa	Kilo Dalton
L	Liter
LN	Lymph node
MDB	Membrane desalting buffer
MEM	Modified eagle medium
mg	Milligram
MgCL ₂	Magnesium chloride
min	Minutes
ml	Milliliter
M-MLV	Moloney murine leukemia virus
nm	Nanometer
MMP	Matrix metalloproteinase
MTA	Metastasis associated gene
MVD	Microvessel density
NaCL ₂	Sodium chloride
NSCLC	Non-small cell lung cancer
NTP	Nucleoside triphosphate
NuRD	Nucleosome remodeling and deacetylation complex
°C	Grad Celsius
PAGE	Polyacrylamide gel electrophoresis
PBS	Phosphate buffered saline
PBST	PBS-Tween
PCNA	Proliferating cell nuclear antigen
PDAC	Pancreatic ductal adenocarcionma
pmol	Picomolar
PP	Percentage of positive stained cell
PVDF	Polyvinylidene difluoride
RCT	Randomized controlled trial
rDNase	Recombinant DNase
RNA	Ribonucleic acid

Abbreviations

RPMI	Roswell park memorial institute medium
RT-PCR	Reverse transcription and polymerase chain reaction
PCR	Polymerase chain reaction
SDS	Sodium dodecyl sulfate
SERM	Selective estrogen-receptor modulator
SI	Staining intensity
TAE	Tris-acetic-EDTA buffer
TBS	Tris-buffer-saline
TBST	TBS-Tween
TEMED	Tetramethylethylenediamine
TGF- β	Transforming growth factor-Beta
Tris	Trizma base
TKI	Tryosine kinase inhibitor
TNM	Tumour, lymph nodes, metastasis
U	Unit
UICC	Union for international cancer control
VEGF	Vascular endothelial growth factor
μ g	Microgram
μ l	Microliter

Summary

Human PDAC is one of the most devastating diseases without effective therapy strategy so far. Although PDCA may not directly depend on estrogen, it was found to be an estrogen-related malignancy. In breast cancer, ligand-activated ER α moves from the cytoplasm to the nucleus of cancer cells, increases the expression of MTA3 and modulates EMT via the transcription factor Snail and the adhesion molecule E-cadherin. To date, this EMT-related signaling pathway has not been investigated in human PDAC. In this study, the prior knowledge about the expression patterns of ER α and the downstream regulation elements MTA3, Snail, and E-cadherin in human PDAC tissues, human pancreatic cancer cell lines and the corresponding xenograft animal model were studied. The results indicated that ER α , MTA3, Snail, and E-cadherin were present in human PDAC tissues, with most of ER α expression in the cytoplasm of the tumor cells instead of the nucleus. The expression patterns of these factors in 5 human pancreatic cancer cell lines, ASPC-1, Capan-1, HPAF-2, MiaPaCa-2 and PANC-1, and the human breast cancer cell line MCF-7 as a control was investigated in the next step. At mRNA level, all cell lines displayed ER α expression, at the protein level only weak expression was detected in the cytoplasm as well as in the nucleus of pancreatic cancer cells due to estrogenic stimulation in the cell culture media. The pancreatic cancer cell line Capan-1 displayed the expression patterns of all factors related to this pathway and will be used for further functional studies. The xenograft animal model of the five human PDAC cell lines showed similar expression patterns compared to the results of the cell culture experiments. In conclusion, the elements of the ER α mediated pathway are present in human pancreatic cancer cells, but the function remains unclear. Most of the ER α is detectable in the cytoplasm of human PDAC at an inactivated form, probably due to a lack of estrogen in the surrounding tissue. Based on these results, further experiments will be done to investigate the role of this signal pathway in mediating EMT in human pancreatic cancer cells.

Zusammenfassung

Das duktales Adenokarzinom des Pankreas ist eine der verheerendsten Erkrankungen, für die es bisher keine effektive Behandlungsstrategie gibt. Obwohl es nicht direkt Östrogen-abhängig ist, wurde gezeigt, dass es ein Östrogen-assoziiertes Tumor ist. Bei Brustkrebs bewegt sich liganden-aktivierter ER α aus dem Zytoplasma zum Zellkern von Tumorzellen, erhöht die Expression von MTA3 und moduliert die Epitheliale-Mesenchymale-Transformation (EMT) über den Transkriptionsfaktor Snail und das Adhensionsmolekül E-Cadherin. Bisher wurde dieser EMT-assoziierte Signalweg noch nicht im duktales Adenokarzinom des Pankreas untersucht. In dieser Arbeit wurde zunächst das Expressionsmuster von ER α und der folgenden Regulationselemente MTA3, Snail und E-Cadherin in menschlichem Pankreaskarzinomgewebe, humanen Pankreaskarzinomzelllinien und dementsprechenden Xenograft Tiermodellen untersucht. Die Ergebnisse zeigten, dass ER α , MTA3, Snail und E-Cadherin in humanem Pankreaskarzinomgewebe vorhanden waren, wobei die höchste ER α -Expression im Zytoplasma zu finden war und nicht im Zellkern. Die Expressionsmuster dieser Faktoren in den 5 humanen Pankreaskarzinomzelllinien ASPC-1, Capan-1, HPAF-2, MiaPaCa-2 und PANC-1 und in der humanen Brustkrebszelllinie MCF-7, als Kontrolle, wurden im nächsten Schritt untersucht. Auf mRNA-Ebene zeigten alle Zelllinien ER α Expression, auf der Proteinebene konnte jedoch nur eine schwache Expression im Zytoplasma und Nukleus festgestellt werden. Die Expression des ER α im Nukleus lässt sich wahrscheinlich durch das östrogenhaltige Zellkulturmedium erklären. Die Pankreaskarzinomzelllinie Capan-1 zeigte die Expression aller zu diesem Signalweg gehörigen Faktoren und wird für weitere funktionelle Untersuchungen verwendet. Das Xenograft Tiermodell der 5 benannten humanen Pankreaskarzinomzelllinien zeigte ähnliche Expressionsmuster wie in den Ergebnissen der Zellkulturexperimente. Zusammenfassend sind die Elemente des ER α -abhängigen Signalwegs in humanen Pankreaskarzinomzellen vorhanden, jedoch bleibt Ihre Funktion unklar. Das meiste ER α findet sich im Zytoplasma in einer inaktivierten Form, wahrscheinlich auf Grund eines Östrogenmangels im umgebendem Gewebe. Basierend auf diesen Ergebnissen werden weitere Experimente durchgeführt werden, um die Rolle dieses Signalwegs bei der Vermittlung von EMT in humanen Pankreaskarzinomzellen zu untersuchen.

1 Introduction

1.1 Pancreatic ductal adenocarcinoma - pathogenesis, therapy and outcome

Pancreatic ductal adenocarcinoma (PDAC) ranks 9th among newly reported cases of cancer and is the 4th most common cause of cancer-related deaths in developed countries. In 2008, the estimated incidence of PDAC was here 165,100 cases with estimated 161,800 deaths from PDAC [1, 2]. PDAC is difficult to diagnose due to a lack of early symptoms because unambiguous symptoms usually appear only at advanced stages. Due to the aggressive pathophysiology including early metastasis, local infiltration especially to nearby neural sheaths, and due to high resistance to chemo- and radiotherapy, the prognosis of PDAC remains poor with an overall 5-year survival rate of just 1–4% [1, 3]. The majority of patients (80–90%) diagnosed at advanced stage with local infiltration or systemic metastasis only reach a median survival period of up to 6 months even after aggressive therapeutic regimens [4].

Surgery with tumor-free margins (R0) offers the only chance to cure this devastating disease for patients with resectable PDAC, but successful R0 resection is achieved in only 30–40% of pancreatectomies with a median survival of 14–20 months [5, 6]. Depending on the location of the tumor, the surgical procedure involves pancreatoduodenectomy, distal or total pancreatectomy. However, surgical treatment alone is no longer sufficient even in patients with radical organ resection. Adjuvant approaches including chemotherapy, radiotherapy and/or molecular target therapy are required and implemented in the treatment of PDAC patients after operation [4].

Chemotherapy plays an indisputable role in the treatment of advanced PDAC. For patients with advanced PDAC, improving patients' quality of life is the main therapeutic goal. There are a variety of agents such as 5-fluorouracil (5-FU), cyclophosphamide, methotrexate, vincristine, and gemcitabine that have been used as chemotherapy for PDAC [7]. Gemcitabine has been proven to be more effective than other drugs as a single agent and is widely accepted as the first choice of chemotherapy for patients at advanced stage [8]. The combination of 5-FU, leucovorin, irinotecan, and oxaliplatin (Folfinox) shows survival benefits in advanced PDAC [9]. Combination of radio- and chemotherapy does not improve the outcome for patients with advanced PDAC compared to chemotherapy alone [10]. This rather traditional adjuvant approach only slightly increased the survival rates of PDAC patients within the last 20 years. Thus, molecular target therapy has

emerged as a new strategy for PDAC.

Molecular target therapy has recently been introduced as a new approach in the treatment of PDAC and has become increasingly important due to the deeper insights into mechanisms and related molecular events involved in PDAC. Molecular therapies target different phases of PDAC development, including tumor initiation e.g. by inhibiting cyclooxygenase 2 using celecoxib [11] and tumor progression e.g. by cetuximab, a monoclonal antibody specific for the epidermal growth factor receptor (EGFR) [4]. Metastatic tumor growth depends upon nutrients provided by newly formed blood vessel. So anti-angiogenic therapy mainly targets the vascular endothelial growth factor (VEGF) should starve the tumor. In a randomized study, marimastat, a monoclonal antibody specific for VEGF improved the 1-year survival rates compared with traditional treatment metastatic PDAC but had no influence on the overall survival rate [12]. Erlotinib has been developed to inhibit the EGFR tyrosine-kinase, which is believed to be responsible for proliferation, angiogenesis, invasion, metastasis, and inhibition of apoptosis of cancer cells [13]. When combined with gemcitabine, which inhibits a family of tyrosine kinases with similar structure, the combination of erlotinib and gemcitabine has been reported to be superior to gemcitabine alone with regard to 1-year survival and tumor control rates in advanced PDAC [4].

These first results of molecular target therapy have so far not been fully satisfying in terms of therapeutic efficacy but point to the direction for obtaining a better prognosis for this devastating disease. They taught us that deeper insights to the mechanisms involved in tumor initiation and progression of PDAC are the key to improve molecular target therapy.

1.2 Epithelial mesenchymal transition and metastatic potential

Epithelial-mesenchymal transition (EMT) was described as a process that enables epithelial cells to undergo a morphological change from cobblestone epithelial phenotype to flat and spindle-shaped mesenchymal phenotype [14]. This process is characterized by degradation of the basement membrane, loss of baso-apical polarization and of cell-cell adhesion [15, 16]. The cells finally gain some mesenchymal capacities, which enable them to go through the membrane and migrate away from the epithelial layer [15]. Multiple changes happens during this transition including enhanced migratory capacity and greatly increased production of extracellular matrix components [17]. EMT has originally been

introduced to describe cellular remodeling during heart morphogenesis and has until now been observed in a variety of physiological and pathological processes even after completion of embryogenesis. Three subtypes of EMT have been divided according to their different biological functions: type 1, EMT during implantation, embryogenesis and organ development; type 2, EMT associated with wound healing and organ fibrosis and type 3, EMT associated with cancer progression and metastasis, the so called cancerous EMT [14].

Cancerous EMT is believed to mark the onset of cancer and to be critical for tumor initiation and tumor progression. The epithelial carcinoma cells change to the mesenchymal phenotype during EMT and gain capacities for invasion [18]. Many important EMT regulators such as the expression of the transcription factors Snail, Slug, and Twist have been shown to correlate with the prognosis in several cancer entities demonstrating that activation of EMT leads to a poor clinical outcome [19]. Cancer cells such as from colorectal cancer, urothelial carcinoma, head and neck squamous cell carcinoma and non-small cell lung carcinoma undergoing EMT become more resistant to drugs [20-22]. Moreover, human cancer cells gain some stem cell-like features during EMT leading to a higher potential for metastasis and drug resistance [23].

Although EMT is acknowledged to be crucial in epithelial cell-derived cancer, the full spectrum of EMT-related or -dependent mechanisms involved is still unclear. Most of the EMT signaling pathways associated with cancer progression seem to converge on E-cadherin, a cell adhesion molecule. Loss of E-cadherin expression and up-regulation of several E-cadherin repressors, such as Snail, Slug, Zeb 1/2, and Twist have been found to promote EMT [24, 25]. Here the zinc-finger transcription factor Snail is believed to be the most important transcription factor; it is overexpressed in the invasive front of breast cancer and inversely correlates with E-cadherin [26]. Similar associations between Snail and E-cadherin have been found in colorectal cancer [27], non-small-cell lung carcinoma [28], gastric cancer [29], endometrial cancer [30] and in PDAC [31].

Signaling pathways recruited by cytokines and growth factors have been demonstrated to regulate Snail and E-cadherin in cells from PDAC. Suppression of the EGFR expression significantly inhibit EMT in pancreatic cancer cells by downregulation of the transcription factors Snail and Slug [32]. As observed in invasive and metastatic PDAC, Kras promotes the metastatic potential in pancreatic cancer cells by downregulation of E-cadherin expression [33]. Transforming growth factor (TGF) β activates EMT also by downregulation of E-cadherin [34]. The co-regulators of EMT, Snail and E-cadherin, are

also involved in signaling by ER α in cells from breast cancer [35]. These results provide us an interesting idea that steroid hormone plays an important role in governing cancerous EMT.

1.3 Estrogen and estrogen receptor α in cancerous EMT

17 β -estradiol is the most potent, biologically active form of the three estrogen variants: estrone, 17 β -estradiol and estriol. Estrogen mediates a broad range of physiological functions as well as pathological processes via cellular receptors, the estrogen receptor alpha (ER α) and estrogen receptor beta (ER β). Both estrogen receptors have five functional domains and share a significant overall sequence homology at DNA level [36].

Estrogen receptors are distributed to a different extent in a variety of tissues. ER α is mostly expressed in liver, breast and uterus, whereas ER β could be detected in tissues of the gastrointestinal tract [37]. In cancer tissues with both ERs expression, they reveal different, sometimes opposite functions [38, 39]. ER α mediates a proliferative effect in the developing breast cancer, while ER β protects from the modulating effects of ER α on cell growth [39].

ER α is a known transcription regulator governing tumor initiation and tumor progression directly by estrogen-regulated target genes [40]. Besides this, there is evidence of cross-talk between ER α and other signal pathways including those involved in EMT. In breast cancer, which is the most extensively investigated cancer type, the estrogen-activated ER α signaling pathway supports an epithelial phenotype of the cancer cells and suppresses EMT [41]. Decreased estrogen dependency correlates with the increase of Snail expression and activity [42]. In vulvar carcinogenesis, downregulation of ER α correlates with a reduction in the expression of E-cadherin compared to normal epithelium [43]. In ovarian cancer, 17 β -estradiol triggers metastatic potential induced by EMT via ER α [44].

Although PDCA may not directly depend on estrogen, it was found to be estrogen-related [38, 45]. Increased exposure to estrogen during the reproductive years is suggested to play a role in the development of PDAC in women [45]. Pancreatic cancer cells are estrogen-sensitive and express both forms of the estrogen receptor. As also reported for breast cancer [39], the ER β /ER α ratio is involved in pancreatic cancer cell growth [38]. Also, several phase II clinical trials report using combination regimens including

chemotherapy agents plus tamoxifen, an estrogen receptor antagonist, to treat PDAC [46, 47]. These trials demonstrate an improvement in the therapeutic effect with a good toxicity profile [46, 47].

The full stream of how ER α mediates biological processes via cellular receptors remains unclear. Upon associating with a heat shock protein ER α is physiologically inactive in the cytoplasm. After binding with its ligand estrogen which enters the cell by simple diffusion, the heat shock protein dissociates from the receptor, two cytoplasmic ER α molecules dimerize and translocate into the nucleus. This complex binds to estrogen-responsive elements (ERE) and activates target gene expression [48]. Several co-activating and co-repressing proteins interact with ER α to modulate the transcriptional process by activating the nucleosome remodeling/histone deacetylase (NuRD) complex [49]. MTA proteins, which are thought to be tightly associated with NuRD, are involved in the signaling process governing cancerous EMT regulated by ER α [35, 50]. It would be interesting to elucidate the expression and role of MTA protein in the cancerous EMT in pancreatic cancer.

1.4 Metastasis-associated gene/protein 3 in cancerous EMT

MTA is a family of genes and their encoded products are associated with cancer progression and metastasis. The three so far known genes *MTA1*, *MTA2*, and *MTA3* encode for 6 reported isoforms of encoded proteins MTA1, MTA1s, MTA1-ZG29p, MTA2, MTA3, and MTA3L [51]. MTA1 are predominantly located in the nucleus, while MTA3 is located in both the nucleus and cytoplasm of tumor cells [35, 52]. MTA proteins are thought to mainly be transcriptional corepressors functioning via histone deacetylation by the NuRD complexes [53].

MTA3, the latest addition to the MTA family, was found to be expressed as well as ER α in several malignant diseases like breast cancer and endometrioid adenocarcinoma. Low expression of MTA3 is a risk factor for breast cancer [54]. In endometrioid adenocarcinoma, downregulation of MTA3 expression predisposes cancer cells to having a high metastatic potential associated with poor differentiation [55]. MTA3 is also a predictor in B-cell lymphoma 6 protein-mediated lymphomagenesis in germinal center B-cell-like neoplasms [56].

The role and function of MTA3 in cancerous EMT is mainly investigated in

estrogen-related breast cancer via ER α [35]. MTA3 highly expressed in epithelial cells of normal tissues is associated with the expression of Snail, E-cadherin and the suppression of EMT. Downregulation of MTA3 has been observed in conjunction with increased malignant potentials of the respective cells. Thus, MTA3 together with ER α functions to maintain a differentiated epithelial status and suppresses EMT [57]. Despite the known expression of estrogen receptors in PDAC, so far there are no reports on MTA3 in this cancer entity.

1.5 Hypothesis and question

ER α seems to be essential for MTA3 expression. What is the experimental evidence? In breast cancer, ligand-activated ER α binds to *MTA3* promoter that contains three potential ERE half-sites in the presence of estrogen and leads to increased expression of MTA3 [35, 50]. ER activates the transcription of MTA3 and forms a transcriptional corepressor complex containing histone deacetylase and ATP-dependent chromatin remodeling functions. This complex is dedicated to *Snail* repression, results in a decreased expression of Snail and an increased expression of E-cadherin (Figure 1) [35]. Thus MTA3 is a downstream receptor of ER α that upon interaction with ER α modulates EMT via Snail and E-cadherin [35, 57].

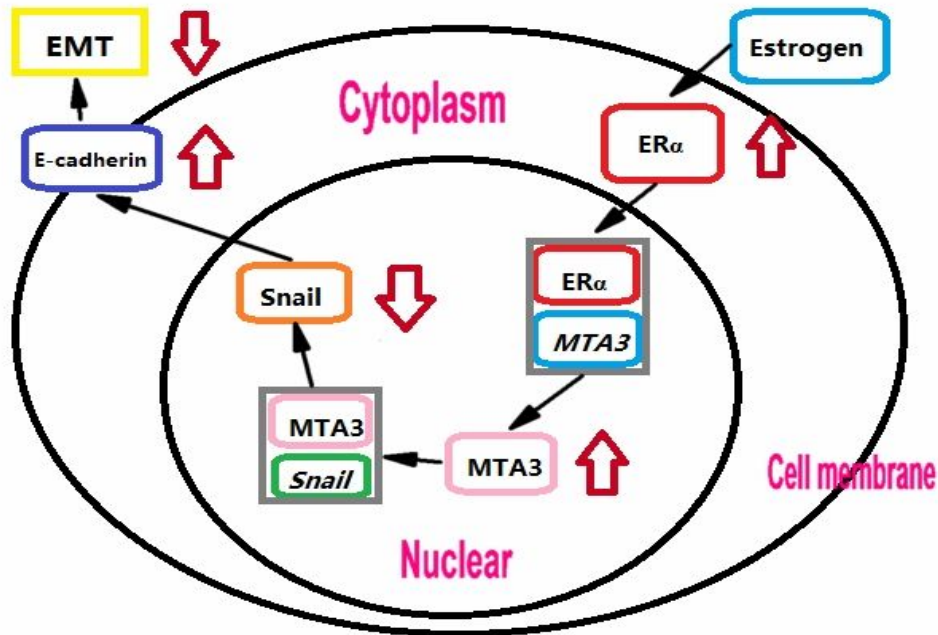


Figure 1. Schematic overview of the relation of ER α and MTA3 in the estrogen-dependent signaling pathway modulating EMT in cancer cells. After 17 β -estradiol binding to cytoplasmic ER α the whole complex enters the nucleus and binds to the ERE of the *MTA3* promoter. Resulting MTA3 blocks the expression of the transcriptional repressor Snail, resulting in an increase of the cell adhesion molecule E-cadherin and subsequent suppression of EMT (according to [35, 50]).

The hypothesis was that estrogen regulates the metastasis-related onset of EMT in primary human PDAC via ER α -dependent MTA3 induction. This assumed that i.e. interference with the estrogen/ER α interaction might reduce the metastatic potential of primary PDAC offering a novel strategy to supplement PDAC therapy. Testing potential effects of estrogen/17 β -estradiol in PDAC, requires prior knowledge of the expression patterns of ER α , MTA3, Snail and E-cadherin as major players of the EMT-related signaling pathway. Aiming to elucidate these patterns, the following questions were experimentally addressed:

1. Do tumor cells of primary and/or metastatic human PDAC express ER α and the downstream regulation elements MTA3, Snail, and E-cadherin?
2. Which human pancreatic cancer cell line represents primary and/or metastatic PDAC with respect to the whole EMT-related signal cascade comprising the estrogen receptor form ER α , the metastasis-associated protein MTA3, the master regulator of EMT Snail and the cell adhesion molecule E-cadherin?
3. Does a xenograft animal model of human PDAC reflect the EMT-related patterns of ER α -dependent proteins in primary and/or metastatic human PDAC?

2 Material and Methods

2.1 Material

2.1.1 Chemicals and Reagents

1 kb DNA ladder RTU	Gene Direx, Aachen, Germany
β-mercaptoethanol	Roth, Karlsruhe, Germany
Acrylamide (40)	Roth, Karlsruhe, Germany
Agarose	Serva, Heidelberg, Germany
Amphotericin B (250 µg/ml)	Biochrom, Berlin, Germany
Antibody dilution buffer	DCS Innovative Diagnostic Systems, Hamburg, Germany
APS	Sigma-Aldrich, Taufkirchen, Germany
Aquatex	Merck, Darmstadt, Germany
Blocking reagent lumilight block	Roche, Mannheim, Germany
Bromphenol blue	Sigma-Aldrich, Taufkirchen, Germany
BSA fraction V	Roth, Karlsruhe, Germany
Coomassie	Sigma-Aldrich, Taufkirchen, Germany
DAB	Sigma-Aldrich, Taufkirchen, Germany
DAPI	Roche, Mannheim, Germany
Disodium hydrogen phosphate dehydrate	Merck, Darmstadt, Germany
DMEM (high glucose 4.5g/L)	PAA, Cölbe, Germany
DMPC	Sigma-Aldrich, Taufkirchen, Germany
dNTP	Sigma-Aldrich, Taufkirchen, Germany
Dream tag master mix	Fermentas, St. Leon-Rot, Germany
EDTA	Sigma-Aldrich, Taufkirchen, Germany
Ethanol (99%)	Merck, Darmstadt, Germany
Ethidium bromide	Roth, Karlsruhe, Germany
FCS (FCS-Gold)	PAA, Cölbe, Germany
Ficoll 400	Sigma-Aldrich, Taufkirchen, Germany
Fluoromount G	Southern Biotech, Eching, Germany
Gelatin	Merck, Darmstadt, Germany

Material and Methods

Glacial acetic acid	Roth, Karlsruhe, Germany
Glycine	Roth, Karlsruhe, Germany
Hematoxylin	Roth, Karlsruhe, Germany
Histokitt-II	Roth, Karlsruhe, Germany
Horse serum	Biochrom, Berlin, Germany
Hydrochloric acid (37%)	Merck, Darmstadt, Germany
Hydrogen peroxide (30%)	Roth, Karlsruhe, Germany
M-MLV reverse transcriptase	Promega, Mannheim, Germany
MEM	PAA, Cölbe, Germany
Methanol (99%)	Roth, Karlsruhe, Germany
Nonfat dry milk	Roth, Karlsruhe, Germany
NucleoSpin II RNA reaction kit	Macherey-Nagel, Düren, Germany
Oligo (dT)	Promega, Mannheim, Germany
Paraformaldehyde	Sigma-Aldrich, Taufkirchen, Germany
PBS	PAA, Cölbe, Germany
Penicillin/streptomycin (100x)	Biochrom, Berlin, Germany
Peq-gold protein marker V	Peqlab, Erlangen, Germany
Peroxidase conjugated avidin biotin complex	KPL, Wedel, Germany
Power block (10X)	BioGenex, Munich, Germany
Protease inhibitor cocktail	Sigma-Aldrich, Taufkirchen, Germany
QuantiPro BCA assay kit	Sigma-Aldrich, Taufkirchen, Germany
Reverse transcription buffer	Fermentas, St. Leon-Rot, Germany
RNAsin	Promega, Mannheim, Germany
RPMI-1640	PAA, Cölbe, Germany
SDS	Roth, Karlsruhe, Germany
Sodium Azid	Sigma-Aldrich, Taufkirchen, Germany
Sodium chloride	Roth, Karlsruhe, Germany
Sodium hydrogenphosphate monohydrate	Sigma-Aldrich, Taufkirchen, Germany
Supersignal West pico chemiluminescent substrate	Thermo Scientific, Schwerte, Germany

TEMED	Sigma-Aldrich, Taufkirchen, Germany
Triton X-100	Sigma-Aldrich, Taufkirchen, Germany
Trizma base	Sigma-Aldrich, Taufkirchen, Germany
Trypsin-EDTA (1x)	PAA, Cölbe, Germany
Tween 20	Roth, Karlsruhe, Germany
Xylazine hydrochloride	Bayer, Leverkusen, Germany
Xylene cyanol F.F	Sigma-Aldrich, Taufkirchen, Germany
Xylol	JT Baker, Griesheim, Germany

2.1.2 Consumable supply

6 well cell culture plate	Greiner, Frickenhausen, Germany
96 well plate	Nunc, Langenselbold, Germany
Cell scraper	Greiner, Frickenhausen, Germany
Collection tube (RNA)	Macherey-Nagel, Düren, Germany
Cover slips (18x18mm, 24x32mm, 40x32mm)	Roth, Karlsruhe, Germany
Glass slides	Paul-Marienfeld, Lauda-Königshofen, Germany
PCR Strips	Biozym, Hess. Oldendorf, Germany
Pipette (2ml, 5ml, 10ml, 25ml)	BD-Falcon, Heidelberg, Germany
Pipette filter tips (0.5–10 μ l, 10–100 μ l, 100–1000 μ l)	Sarstedt, Nümbrecht, Germany
Pipette tips (0.5–10 μ l, 10–100 μ l, 100–1000 μ l)	Sarstedt, Nümbrecht, Germany
PVDF membrane	Thermo Scientific, Schwerte, Germany
Reaction tube (0.5ml, 1ml, 2ml)	Sarstedt, Nümbrecht, Germany
Tissue culture flask (75cm ²)	Sarstedt, Nümbrecht, Germany
Tube (15ml, 50ml)	BD-Falcon, Heidelberg, Germany
UV transparent cuvettes	Sarstedt, Nümbrecht, Germany

2.1.3 Equipment

Camera, canon powershot S515	Canon, Japan
Centrifuge biofuge primo R	Heraeus, Hanau, Germany
Centrifuge megafuge 1.0	Heraeus, Hanau, Germany
Centrifuge minispin	Eppendorf, Hamburg, Germany
Clean bench captair filtair	Erlab, Cologne, Germany
Clean bench clean air	CleanAir, USA
Clean bench HERA safe	Heraeus, Hanau, Germany
CO ₂ incubator HERA cell	Heraeus, Hanau, Germany
Electrophoresis chamber mini-protean	BioRad, Munich, Germany
Electrophoresis chamber sub-cell	BioRad, Munich, Germany
Electrophoresis power supply consort E835	Sigma-Aldrich, Taufkirchen, Germany
Electrophoresis power supply power-pac 1000	BioRad, Munich, Germany
Freezer (-20°C)	Bosch, Stuttgart, Germany
Freezer (-80°C) forma 700 series	Thermo Scientific, Schwerte, Germany
Gel cast chambers	BioRad, Munich, Germany
Heating block thermomixer 5436	Eppendorf, Hamburg, Germany
Incubator herahybrid	Kendro, Hanau, Germany
Luminescence imaging	Peqlab, Erlangen, Germany
Magnetic stirrer SB161	VWR, Darmstadt, Germany
Microscope axioskop 2	Karl-Zeiss, Oberkochen, Germany
Microscope eclipse TS100	Nikon, Düsseldorf, Germany
Microwave	Bosch, Stuttgart, Germany
Multipipettor	Eppendorf, Hamburg, Germany
pH-Meter CG840	Schott- Geräte, Hofeim, Germany
Pipette (0.5–10µl, 10–100µl, 100–1000µl)	Eppendorf, Hamburg, Germany
Pipettor (0.1–200 ml)	Hirschmann, Eberstadt, Germany

Refrigerator	Bosch, Stuttgart, Germany
Rotation microtom RM2125RT	Leica, Solms, Germany
Shaker grant-bio PMR-30	VWR, Darmstadt, Germany
Shaker gyro-rocker SSL3	Sigma-Aldrich, Taufkirchen, Germany
Shaker polymax 1040	Heidolph, Schwabach, Germany
Spectrophotometer microplate reader EL808	Bio-Tek, Bovenden, Germany
TFT LCD color monitor	Kisker-biotech, Steinfurt, Germany
Thermocycler mastercycler gradient	Eppendorf, Hamburg, Germany
UV-plate	Herolab, Wiesloch, Germany
UV/Vis photometer biophotometer	Eppendorf, Hamburg, Germany
Vortex 2 genie	VWR, Darmstadt, Germany
Water bath JR5	VWR, Darmstadt, Germany
Weight BP-3105	Sartorius, Göttingen, Germany

2.1.4 Primers for RT-PCR

ER α (NM_000125.3)	153 bp, annealing temperature, 60°C
Sense	5'-AATgATTCTATAATgCCATCATgCAGC-3'
Anti-sense	5'-gCTTggTTAAACATATCTgCAAaggTTAC-3'
MTA3 (NM_020744)	327 bp, annealing temperature, 58°C
Sense	5'-TgAggCTgAggAggAggC-3'
Anti-sense	5'-CTTCTATCCTTCTTATTAggTATgggTTgC-3'
Snail (NM_005985.2)	228 bp, annealing temperature, 56°C
Sense	5'-gAggCggTggCAGACTAg-3'
Anti-sense	5'-gACACATCggTCAgACCAg-3'
E-cadherin (NM_004360.3)	421bp, annealing temperature, 56°C
Sense	5'-ATTCTgATTCTgCTgCTCTTg-3'
Anti-sense	5'-AgTAgTCATAgTCCggTCTT-3'

The primers were designed with the computer program PRIMER3 and established in the surgical research laboratory, Charité – CBF, Berlin, Germany. The primers were purchased from TIB-Molbiol, Berlin, Germany.

2.1.5 Antibodies

Primary antibodies

ER α	Rabbit polyclonal	Ab-17, RB-1521-P, Thermo Scientific, Schwerte, Germany
MTA 3	Rabbit polyclonal	A300-160A, Bethyl, Hamburg, Germany
Snail	Rabbit polyclonal	H-130, sc-28199, Santa Cruz, Heidelberg, Germany
E-cadherin	Rabbit polyclonal	H-108, sc-7870, Santa Cruz, Heidelberg, Germany
PCNA	Rabbit polyclonal	FL-261, sc-7907, Santa Cruz, Heidelberg, Germany
β -actin	Mouse monoclonal	A-5441, Thermo Scientific, Schwerte, Germany

Secondary antibodies for IHC

Biotinylated goat anti-rabbit IgG	sc-2040, Santa Cruz, Heidelberg, Germany
Goat anti-rabbit IgG-TR (conjugated to Texas Red)	sc-2780, Santa Cruz, Heidelberg, Germany

Secondary antibodies for western blotting

Peroxidase-conjugated anti-rabbit IgG	A-2545, Sigma, Taufkirchen, Germany
Peroxidase-conjugated anti-mouse IgG	A-3526, Sigma, Taufkirchen, Germany

2.1.6 Cell culture media

ASPC-1/ Capan-1/MCF-7	
RPMI 1640	500 ml
FCS (10%)	50 ml
Penicillin/ streptomycin (100X)	5 ml
Amphotericin B (250 µg/ml)	0.5 ml

HPAF-2	
MEM	500 ml
FCS (10%)	50 ml
Penicillin/ streptomycin (100X)	5 ml
Amphotericin B (250 µg/ml)	0.5 ml

MiaPaCa-2	
DMEM	500 ml
FCS (10%)	50 ml
Horse serum	12.5 ml
Penicillin/ streptomycin (100X)	5 ml
Amphotericin B (250 µg/ml)	0.5 ml

PANC-1	
DMEM	500 ml
FCS (10%)	50 ml
Penicillin/ streptomycin (100X)	5 ml
Amphotericin B (250 µg/ml)	0.5 ml

2.1.7 Solutions

2.1.7.1 Commonly used solutions

TBS	in dd water (5000 ml)
Trizma base	30.5 g
NaCL	44 g
Adjust to pH 7.6 with HCL	

0.1% TBST	in TBS (5000 ml)
Tween 20	5 ml

0.5M EDTA pH 8.0	in dd water (500 ml)
EDTA	73.05 g
Adjust to pH 8.0 with NaOH	

2.1.7.2 Solutions for immunohistochemistry

1% gelatin	in dd water (100 ml)
gelatin	1 g
Sterilized by autoclaving	

PBS (0.2M)	in dd water (5000 ml)
NaH ₂ PO ₄ ·H ₂ O (0.2M) (27.6g/1000ml dd water)	28.75 ml
Na ₂ HPO ₄ ·2H ₂ O (0.2M) (35.6g/1000ml dd water)	96.2 ml
NaCL	22.4 g
Adjust pH to 7.4 with HCL	

Material and Methods

0.1% PBST	in PBS (5000 ml)
Tween 20	5 ml

0.01% EDTA pH 8.0	in dd water (500ml)
0.5 M EDTA pH 8.0	340 µl

1% H₂O₂	in dd water (200 ml)
H ₂ O ₂ (30%)	7 ml

4% paraformaldehyde (pH 7.4)	in PBS (100 ml)
paraformaldehyde	4 g
Store at -20°C	

0.5% Triton x-100	in PBS (100 ml)
Triton x-100	0.5 g

2.1.7.3 Solutions for western blotting

Lysis buffer III for protein extraction	in dd water (100 ml)
1M TRIS-HCL pH 6.8	1 ml
0.5 M EDTA pH 8.0	0.4 ml
0.5 M NaCL	3 ml
Brij 96 (10%)	8.75 ml
Phenylmethylsulfonyl fluoride (10%)	1.25 ml

Running buffer (5x)	in dd water (1000 ml)
Trizma base	15 g
Glycine	72 g
SDS	5 g

Material and Methods

Transfer buffer	in dd water (1000 ml)
Trizma base	3.03 g
Glycine	14.4 g
Methanol (99%)	200 ml

Sample buffer (5x)	(8ml)
0.5 M TRIS-HCL pH 6.8	1.25 ml
10% SDS	2 ml
Glycerol	2 ml
Mercaptoethanol	0.5 ml
Bromphenol blue (0.5%)	0.5 ml
dd water	1.75 ml

0.5 M Tris-HCL pH 6.8	in dd water (100 ml)
Trizma base	6 g
Adjust pH to 6.8 with HCL	

1.5 M Tris-HCL pH 8.8	in dd water (100 ml)
Trizma base	18.15 g
Adjust pH to 8.8 with HCL	

10% Separating Gel	2 mini gels (10ml)
dd water	4.9 ml
Acrylamide (40)	2.5 ml
1.5 M Tris-HCL pH 8.8	2.4 ml
10% SDS	0.1 ml
10% APS	0.1 ml
TEMED	5 μ l

Material and Methods

5% BSA-NaAzid	In PBS 500ml
BSA	25 g
NaAzid	0.5 g

5% Stacking Gel	2 mini gels (5ml)
dd water	3.145 ml
Acrylamide (40)	0.5 ml
0.5 M Tris-HCL pH: 6.8	1.25 ml
10% SDS	0.05 ml
10% APS	0.05 ml
TEMED	5 µl

2.1.7.4 Solutions for RT-PCR

50x TAE buffer	in dd water (1000 ml)
Trizma base	242 g
Glacial acetic acid	57.1 ml
0.5 M EDTA pH 8	100 ml

DNA-loading buffer (6x)	in dd water (10 ml)
Bromphenol blue	0.025 g
Xylene cyanol F.F	0.025 g
Ficoll 400	1.5 g

Agarose gel (1%)	
TAE (1x)	50 ml
Agarose	5 g
Ethidium bromide (1%)	5 μ l
The agarose was dissolved in TAE with heat treatment (microwave), then ethidium bromide was added and filled in a plastic frame. After cooling down to RT, the gel was ready for loading DNA samples and electrophoresis.	

2.1.8 Clinical data of pancreatic cancer patients

26 tissue samples of pancreatic ductal adenocarcinoma were collected at the Institute of Pathology, Charité School of Medicine, Campus Benjamin Franklin (Berlin, Germany). Patients with primary pancreatic adenocarcinoma, who underwent surgery without prior chemotherapy, were enrolled in this study. 15 patients were male and 11 were female. Patients' age ranged from 48–80 years and the median age was 66 years. The TNM stage of the patients according to UICC 1997 (TNM Classification of Malignant Tumors, 5th edition, UICC) and the pathological grading were listed in table 1. All pancreatic carcinoma tissues obtained were fixed in 4% formalin and embedded in paraffin.

Table 1: Clinical and pathological data of pancreatic ductal adenocarcinoma patients

	Cases (n = 26)
Gender	
Male	15
Female	11
Age median (range)	66 (48–80) Years
TNM Stage	
I	2
II	8
III	16
Pathological grading	
Moderate	14
Moderate to poor	6
Poor	6

2.1.9 Cell lines

The human pancreatic cancer cell lines ASPC-1 (poorly to moderately differentiated), Capan-1 (well differentiated), HPAF-2 (moderately differentiated), MiaPaCa-2 (undifferentiated) and PANC-1 (poorly differentiated), as well as the human breast adenocarcinoma cell line MCF-7 were obtained from the ECACC (Salisbury, United Kingdom) and the DSMZ (Braunschweig, Germany).

2.2 Methods

2.2.1 Cell culture and preparation of cells for IHC

The cells were incubated in the medium mentioned above (2.1.6) in an incubator with humidified air containing 5% CO₂ at 37°C. The medium was changed thrice weekly and the cells were maintained by serial passaging after trypsinization with 0.1% trypsin-EDTA

in PBS.

In order to grow human pancreatic cancer cells on cover-slips for IHC, the glass slips were sterilized by autoclaving and separately set into a 6 well cell culture plate. The cover slips were pre-incubated in 2 ml of a 1% gelatin solution in dd water in an incubator at 37°C for 30 min. After removing the remaining gelatin solution, the human pancreatic cancer cells were added into the 6 well cell culture plate and seeded overnight in an incubator with humidified air containing 5% CO₂ at 37°C. The next day, the cells were used for IHC.

2.2.2 Orthotopic nude mouse model for pancreatic cancer

A previously established nude mouse model for human pancreatic cancer was applied for in vivo studies [58]. 10⁵–10⁶ cells of each human pancreatic cancer cell line (ASPC-1, Capan-1, HPAF-2, MiaPaCa-2 or PANC-1) were injected subcutaneously into the flanks of nude mice. The subcutaneous tumors were harvested 3-4 weeks later when the largest diameter of the tumor had reached 1cm, and minced into small fragments of 1 mm³ by a scalpel. Only vital tumor tissue from the outer part of the donor tumor was used for orthotopic implantation. Tumor recipient nude mice were anesthetized, laparotomized with a middle incision and two donor tumor fragments were placed in the parenchyma of the pancreatic tail. The mice were monitored daily for clinical conditions and sacrificed 14 weeks after orthotopic tumor implantation. After obduction of the mice, the primary tumors were harvested, fixed in 4% formalin, and embedded in paraffin. Three-micrometer-thick tissue sections were prepared and stained with hematoxylin and eosin to analyze the tumor structures.

2.2.3 Immunohistochemistry

2.2.3.1 IHC on paraffin-embedded tissues

Three-micrometer-thick sections from human PDAC as well as from orthotopic grown tumors were prepared by using a rotation microtom. The paraffin-embedded sections were deparaffinized with xylol (3 x 5 min), rehydrated in 99% ethanol (2 x 5 min), 96% ethanol (5 min), 70% ethanol (5 min), and rinsed in dd water. Antigen retrieval was performed with

heat treatment (900W, 5 min; 180W, 5 min) in 0.01% EDTA (pH 8.0). The slides were cooled down at room temperature for 25 min followed by rinsing with dd water. To block endogenous peroxidase the tissue sections were treated with 1% hydrogen peroxide for 25 min and rinsed in dd water and PBST for 5 min each. Nonspecific antigens were masked by incubating the tissue sections in 1 x Power Block for 5 min at room temperature. The Primary antibodies (2.1.5) were diluted in antibody dilution buffer (ER α 1:75, MTA3 1:400, Snail 1:50, E-cadherin 1:100, PCNA 1:75) and applied to the tissue sections for 30 min at 37°C. As negative control, sections were incubated with the antibody dilution buffer instead of the primary antibody. After washing with PBST (3 x 5 min) the tissue sections were incubated with biotinylated secondary antibodies (2.1.5) diluted in antibody dilution buffer (1:200) for 30 min at 37°C. Repeated washing with PBST (3 x 5 min), the tissue sections were finally incubated with peroxidase conjugated avidin complex for 30 min at 37°C. After rinsing in TBS (3 x 5 min), a brown color reaction was induced with DAB. The sections were then counterstained with Mayer's hematoxylin and dehydrated with upgraded ethanol (70%, 96% and 99%) for 2 min each. After immersion in xylol for 2 x 5 min, the tissue sections were mounted with Histokitt-II, and analyzed using a standard light microscope.

2.2.3.2 IHC on pancreatic cancer cell lines

After growing overnight on cover-slips, the human pancreatic cancer cells as well as the human breast cancer cells were washed with PBS and fixed in 4% paraformaldehyde in PBS for 15 min at room temperature. After washing with PBST (3 x 5min), the cells were incubated in 0.5% Triton X-100 in PBS for 5 min to enhance the permeabilization of the plasma membrane. Then the cells were treated in the same way as the paraffin-embedded tissue with the primary antibodies (ER α , MTA3, Snail and E-cadherin), secondary antibodies and peroxidase-conjugated avidin complex. After the immunoreaction with DAB, the sections were then counterstained with Mayer's hematoxylin and finally mounted with Aquatex.

For immunofluorescence staining, the same procedure as mentioned above was used, but the secondary antibody was a Texas red-conjugated goat anti-rabbit IgG-TR (1:200) and was applied to the slides for 1 hour at room temperature in the dark. After washing with PBS, the cells were counterstained with DAPI (1:10000) for 10 min covered from light.

Followed by washing with PBS again, finally, the slides were mounted with Fluoromount G and stored at 4°C in the dark.

2.2.3.3 Evaluation of immunohistochemical staining results

Immunohistochemical staining intensity was evaluated by using a semiquantitative method described by Stierer et al [59]. The slides were viewed under a light microscope at HPF (high power field) and 400× magnification. 3 HPF of 3 individual slides were evaluated. Stain intensity (SI): graded as, no staining, 0; weak staining, 1; moderate staining, 2; and strong staining, 3 (Figure 2). Percentage of positive cells (PP) was estimated from 0 to 4: 0 corresponded to <1% positive pancreatic cancer cells, 1, to 1%–10% positive pancreatic cancer cells, 2, to 11%–50% positive pancreatic cancer cells, 3, to 51%–80%, and 4 corresponded to >81% positive pancreatic cancer cells. The immunohistochemical reaction score (IRS) was calculated as follows: $IRS = SI \times PP$. $IRS \leq 1$ was defined as negative and $IRS > 1$ was defined as positive in the human tissues [59].

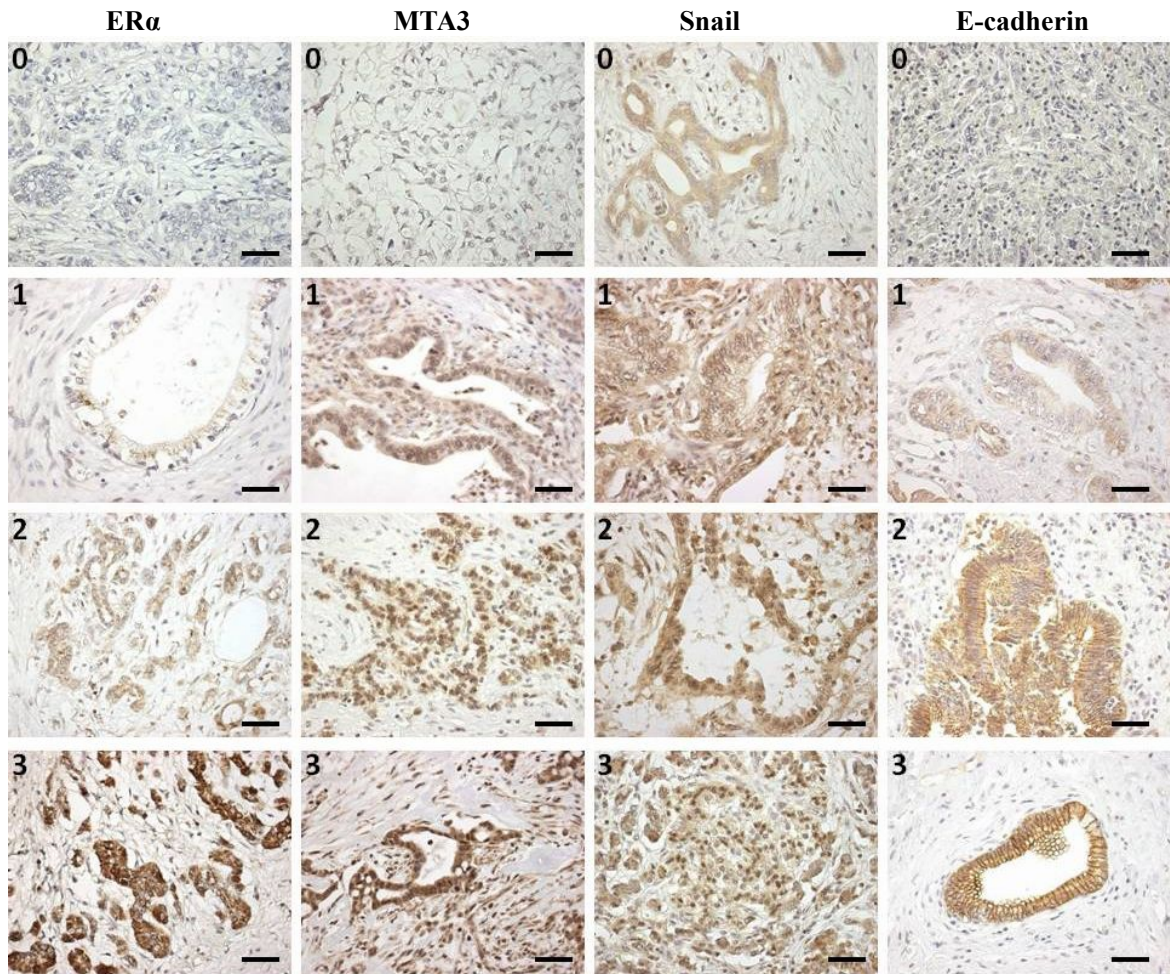


Figure 2: Immunohistochemical staining for ER α , MTA3, Snail and E-cadherin in human primary PDAC tissues. Representative images for the following stainings of FFPE samples (3 μ m) with peroxidase-coupled rabbit specific secondary antibodies: (ER α), cytoplasmatic staining of ER α by rabbit-derived polyclonal anti-human ER α .; (MTA3), nuclear and cytoplasmatic staining of MTA3 by rabbit-derived polyclonal anti-human MTA3. (Snail), nuclear and cytoplasmatic staining of Snail by rabbit-derived polyclonal anti-human Snail. (E-cadherin) E-cadherin in the cell membranes by rabbit-derived polyclonal anti-human E-cadherin. (0 negative, 1 weak staining, 2 moderate staining, 3 strong staining). (scale bars: 250 μ m, original magnification: 400x)

2.2.4 Western blot analysis

2.2.4.1 Protein isolation

Human pancreatic cancer cells cultured in cell culture flasks were washed twice with ice-cold PBS, harvested using a cell scraper, and centrifuged at 1000 rpm for 5 min at room temperature. After repeated washing with ice-cold PBS, the cell pellets were finally resuspended in protein lysis buffer containing 1x protease inhibitor cocktail. The lysates

were incubated on ice on a rotating plate, for 15 min, vortexed, and then centrifuged at 10000 x g for 15 min at 4°C. The supernatant (protein solution) was collected and stored at -20 °C.

2.2.4.2 Determination of protein concentration

Protein concentrations were determined using a BCA assay kit. A negative control as well as serial of BSA solutions diluted in dd water (0.31µg/ml, 0.62µg/ml, 12.5µg/ml, 25µg/ml, 50µg/ml) were used as standard samples to prepare a calibration curve. Protein samples were diluted 1:200 in dd water and 100µl of each solution (protein samples and BSA solutions) was added to a 96-well plate. The reagent mixture for the protein assay was prepared by diluting 50 parts of reagent A and 1 part reagent B. 100µl reagent mixture was added to each well. All probes were run in duplicates. The samples were incubated at 60°C for 1 hour. In the presence of protein, the light green reagent mixture was changing to purple. The absorptions were estimated at 550 nm using a spectrophotometer. The concentrations of the proteins were calculated after interpolated the absorptions to the pre-established linear regression line through the standard points.

2.2.4.3 Electrophoresis and Immunoreactions

Electrophoresis was performed using 10% SDS-PAGE gels. A 10% separating gel (1 mm thickness) and a 5% stacking gel were prepared as mentioned above (2.1.7.3). Using a gel cast chamber, the separating gel was casted first, covered with 70% ethanol and kept at room temperature for 30 min to allow polymerization. The ethanol was then discarded and the stacking gel was casted above the separating gel. A 10-well-comb was inserted into the stacking gel solution to cast wells for loading the protein samples. 50µg protein including 6x loading buffer were denatured at 95°C for 5 min and placed on ice immediately to avoid renaturation of the proteins. After a slight spin down (3000 rpm x 30 seconds) at room temperature, the samples were loaded on the gel, 3µl of a protein marker (10–250 kDa) was used for estimating the size of the proteins. The electrophoresis was run at 100V in 1x running buffer for about 2 hours, until the blue loading buffer had almost reached the bottom of the gel. A PVDF membrane was used for blotting the protein. After activating the PVDF membrane in 99% methanol for 3-5 seconds and 5 min equilibration in transfer

buffer, a “sandwich blot” was built as described in Figure 3.



Figure 3: The “sandwich blot” for protein samples blotted electrophoretically to a PVDF membrane. “+” referred to the positive electrode, “-” represented the negative electrode. After building the electrophoretical field the proteins are moving from the “-” to the “+” field as the red arrow indicates, and were finally stopped by the PVDF membrane.

The proteins were transferred to the PVDF membrane by 1 hour electrophoretic transfer at 100V in ice cold transfer buffer. The transfer was accomplished in an ice-cooled chamber on a magnetic stirrer to decrease lateral diffusion of protein due to warming of the buffer. To estimate the protein transferred to the membrane after blotting, the pre-stained marker was used to make sure that every band had transferred clearly and completely. For further testing, the gel was stained with coomassie for 5 minutes to detect proteins which were still remaining in the gel. The membrane was now ready for the immunoreactions. To block non-specific antigens, the membranes were incubated with 3% nonfat dry milk in TBS for 2 hours at room temperature on a rotating plate. The primary antibodies (2.1.5) were diluted in 5% BSA-NaAzid in TBS (ER α 1:200, MTA3 1:500, Snail 1:200, E-cadherin 1:500) and the membranes were exposed to the primary antibody at 4°C overnight on a rotating plate. After repeated washing with TBST (3 x 15 min), the membranes were incubated for 2 hours with peroxidase-linked secondary antibody (2.1.5) in 1% lumi-light blocking reagent in TBS (1:1000) at room temperature on a rotating plate. Finally after repeated washing with TBST (3 x 15 min), the membranes were exposed to SuperSignal West Pico Stable Solution and SuperSignal West Pico Luminol/Enhancer Solution(1:1) for 5 min to activate the chemiluminescence signal. The membrane was applied to a luminescence imaging system and the signals were visualized on a computer.

2.2.5 Reverse transcription and polymerase chain reaction

2.2.5.1 RNA isolation and determination of RNA concentration

Total cellular RNA was extracted from cells using the NucleoSpin RNA II kit according to the manufacturer's instructions. The human pancreatic and breast cancer cells were washed twice with ice-cold PBS and harvested after trypsinization with 0.1% trypsin-EDTA in PBS. After centrifugation at 1000 rpm for 5 min at room temperature, the cell pellet was resuspended in lysis buffer solution (350µl lysis buffer RP1 + 3.5µl β-ME). After clearing the lysates by filtrating using NucleoSpin® filter columns and precipitating the ions by mixing the lysates with 350µl 70% ethanol, the RNA was bound on a silica membrane provided with the RNA extraction kit. The membrane was then desalted by MDB and incubated with 95 µl rDNase reaction mixtures (10 µl rDNase + 90 µl reaction buffer) for 15 min at room temperature to digest remaining DNA.. After washing with 200µl washing buffer RA2, 600µl and 250µl RA3, the RNA was finally eluted in a suitable volume of RNase-free water in a reaction tube and stored at -80°C. RNA concentration was determined using a BioPhotometer. 1µl RNA was diluted in 99µl DMPC water, and at an absorption of 260/280 nm, the RNA concentration could be calculated.

2.2.5.2 Reverse transcription from RNA to cDNA and PCR conditions

Samples containing 2 µg RNA and DMPC water in a total volume of 16µl were incubated at 70°C for 5 min. 1µl oligo (dT), 1µl M-MLV-RT, 1µl dNTP (dATP, dCTP, dGTP and dTTP) and 5µl 5 x reaction buffer were added to each sample and the samples were incubated in a Thermocycler at 37°C for 1 hour for cDNA synthesis and at 70°C for 15 min to denature reverse transcriptase. The cDNA were then stored at -20°C.

First-strand cDNA was amplified with transcript-specific oligonucleotides (ERα, Snail, MTA3 and E-cadherin listed in 2.1.4) using 2x DreamTaq master mixture containing 0.05U/µl Taq DNA polymerase, dNTP 0.4 mM each and 4 mM MgCl₂. The primers (10 pmol/µl) for the respective genes were already established (2.1.4) and the reaction mixtures were prepared as described in Table 2:

Table 2: Reaction mixture of RT-PCR

	Volume
cDNA	2 μ l
Primer sense	1 μ l
Primer antisense	1 μ l
PCR reaction Mixture (Dream Taq) (2X)	12.5 μ l
DMPC H ₂ O	9.5 μ l
Total volume	25 μ l

The PCR program was accomplished as described in Table 3, First, the samples were incubated at 93°C for 1 min for initial denaturation to separate the DNA strands, then 36 reaction cycles including denaturation, annealing, and extension phase were proceeded. The oligonucleotides anneal to the DNA strands when the temperature decreased and the Taq polymerase finally synthesized the complementary strands using dNTP in the extension phase at 72°C. The annealing temperature was calculated according to specify the different primers (2.1.4).

Table 3: PCR conditions

Stage	Temperature	time
1. Initial denaturation	93°C	3 min
2. Denaturation	93°C	1 min
3. Annealing	56°C–60°C	1 min
4. Extension	72°C	40 seconds
5. Return to 2. and repeat, for another 35 cycles		
6. Final extension	72°C	10 min
7. Storage	4°C	

A 1% agarose gel in TAE containing 0.1% ethidium bromide was used for separating the DNA fragments electrophoretically. 5 μ l 6x loading buffer was added to (how much) each sample and a 1 kb DNA molecular weight marker was used to determine the length of the DNA fragments. After electrophoresing at 80V for about half an hour, the DNA fragments were visualized and photographed under UV light and photographed with a digital camera.

2.2.6 Statistic analysis

The Mann-Whitney U test (group=2) or (sprcify) Kruskal-wallis test (group=3) was used to compare the means of the different IRS. The non-parametric Spearman correlation coefficient test was used to evaluate correlations between MTA3, Snail and E-cadherin (SPSS 13.0). Statistic significance was assumed at $p < 0.05$.

3 Results

3.1 Localization of molecules of the ER α signaling pathway and proliferation in primary human PDAC tissues *in-situ*

3.1.1 ER α

Addressing the potential relevance of ER α -mediated effects in pancreatic cancer, expression patterns for ER α , related signaling molecules as well as local proliferation of cancer cells were examined by immunohistochemistry in 26 human PDAC tissue samples obtained from patients with primary human pancreatic cancer.

All PDAC tissues were characterized by abnormal glandular structures embedded in desmoplastic stroma. Well differentiated PDAC comprised large duct-like structures with low mitotic activity as defined by large round to ovoid nuclei with sharp nuclear membranes. Moderately differentiated PDAC showed a mixture of medium-sized duct-like and tubular structures of variable shapes as well as marked mitosis also with regard to greater variation in nuclear size and chromatin structure than that observed in well differentiated PDAC. Poorly differentiated PDAC were composed of small irregular glands as well as solid tumor cell sheets and nests, while no acinar tissues or duct-like structures were found. The neoplastic cells of poorly differentiated PDAC showed marked pleomorphism and considerable mitotic activity. [60]

Specific immunohistochemistry identified the ER α in both the nucleus and in the cytoplasm of cancer cells (Figure 4). As for the typical picture in human PDAC tissues, ER α staining was detected in the cytoplasm in 96% (25/26) of the cases (Figure 4A). Only in the samples of one male patient, ER α was found in the nucleus (Figure 4B). Intensity and localization of immunostained ER α did not depend on the patient's gender, differentiation status of the PDAC, disease stages or nodal status (Table 4). However, ER α was mostly observed in the cytoplasm of well differentiated duct-like structures in human PDAC tissues, while only a weak immunoreaction was detected in surrounding cancerous stroma cells. In noncancerous pancreatic tissues, acinar, duct-like cells and islet cells showed ER α expression that was stronger than that observed in the cancerous areas of the same tissue sample (Figure 4C). These results indicated that ER α existed in human PDAC tissues as well as in noncancerous pancreatic tissues.

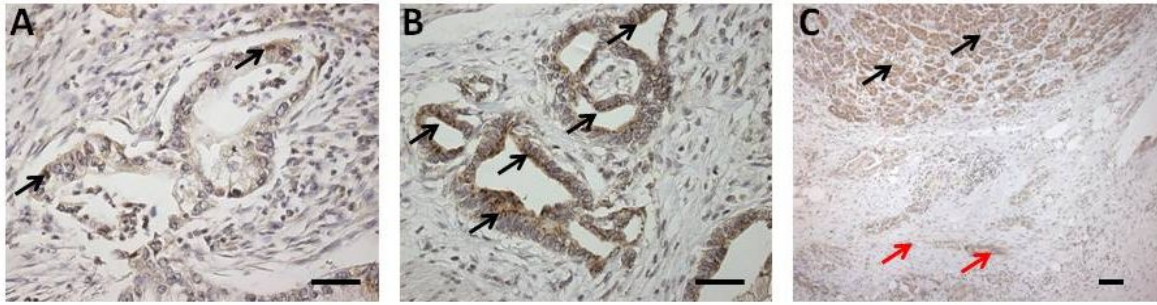


Figure 4: Immunohistochemical staining for ER α in human primary PDAC tissues. Formalin-fixed paraffin-embedded (FFPE) samples (3 μ m) of human PDAC tissue were stained with rabbit-derived polyclonal anti-human ER α . Primary antibody binding was detected using a peroxidase-coupled rabbit specific secondary antibody. ER α ⁺ cells appear in brown staining (arrows). Representative images show (A) cytoplasmatic (25/26) and (B) nuclear localization of ER α (1/26) (scale bars: 250 μ m, original magnification: 400x). (C) Comparison of cytoplasmatic expression in noncancerous (black arrows) and cancerous areas of pancreatic tissues (red arrows). (scale bars: 250 μ m, original magnification: 200x)

3.1.2 MTA3, Snail and E-cadherin

Having demonstrated that ER α was present in human PDAC tissue, these tissues were also tested for the downstream molecules MTA3, Snail and E-cadherin (Figure 5).

MTA3 was mostly found in the nucleus as well as in the cytoplasm of those duct-like pancreatic cancer cells in human PDAC tissue, where immunohistochemical staining also detected cytoplasmatic ER α (Figure 5). In 50% (13/26) of all human PDAC tissues, MTA3 was discovered in the nucleus of human PDAC cells, mostly located in the well differentiated duct-like structures with expression of ER α . While 64% (9/14) of the patients with moderately differentiated PDAC showed positive MTA3 staining, only 33% (4/12) of moderately to poorly differentiated or poorly differentiated PDAC comprised MTA3⁺ cells. MTA3 expression in lymph node-negative patients (60%; 6/10) was higher than that found in lymph node-positive patients (44%; 7/16). However, when compared with IRS (immunohistochemical reaction score) or PP (percentage of positive cells), no significant correlation was found between the expression of MTA3 and the PDAC differentiation status, UICC stages or nodal status (Table 4).

Snail was found in the nucleus and cytoplasm of duct-like pancreatic cancer cells in 77% (20/26) of all human PDAC tissues (Figure 5). Poorly differentiated PDAC tissues showed more Snail (100%; 6/6) than moderately (64%; 9/14) or moderately to poorly differentiated PDAC tissues (83%; 5/6). Again, these differences did not reach significance when compared with IRS or PP, and no correlation was found between Snail and UICC or nodal status (Table 4).

E-cadherin expression was detected in well differentiated duct-like structures of 77% (20/26) of all of the human PDAC tissues with variable degrees of membrane staining (Figure 5). Expression of E-cadherin was stronger with advanced tumor differentiation, i.e., it was found in 93% (13/14) of moderately differentiated, 100% (6/6) of moderately to poorly differentiated and only 17% (1/6) of poorly differentiated human PDAC tissues. The IRS ($p=0.018$) and PP ($p=0.010$) reached significance among these three groups (Table 4). No difference was found in the correlation between E-cadherin expression and UICC stages or lymph node metastasis status (Table 4).

As shown here, MTA3, Snail and E-cadherin were determined in human PDAC tissues.

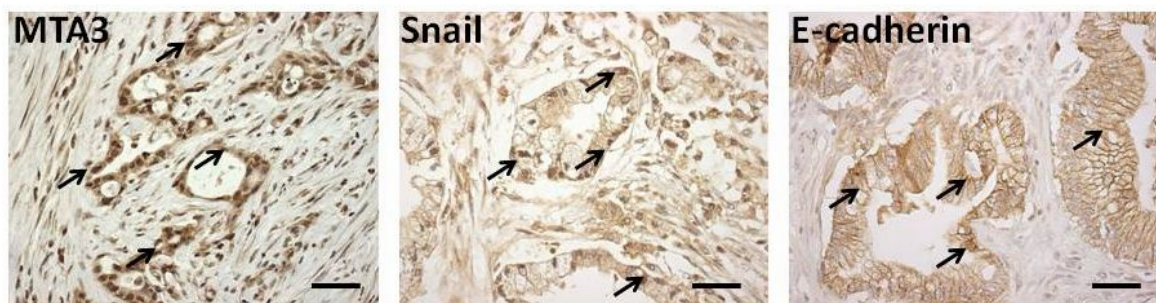


Figure 5: Immunohistochemical staining for MTA3, Snail and E-cadherin in human primary PDAC tissues. Representative images for the following staining of FFPE samples (3 μm) with peroxidase-coupled rabbit specific secondary antibodies: (A) Nuclear MTA3 by rabbit-derived polyclonal anti-human MTA3 (13/26). (B) Nuclear Snail by rabbit-derived polyclonal anti-human Snail (20/26). (C) E-cadherin in the cell membranes by rabbit-derived polyclonal anti-human E-cadherin (20/26). Arrows mark positive cells. (scale bars: 250 μm , original magnification: 400x)

Table 4: Correlation between expression of ER α (cytoplasm), MTA3, Snail or E-cadherin determined as IRS or PP to UICC (I-III), PDAC differentiation (moderately [M], moderately to poorly [M to P] and poorly differentiated [P]) or lymph node metastasis stages (N(0-1)). Statistical comparisons were done using the Kruskal-Wallis test for independent samples. (*:p<0.05) (IRS: immunohistochemical reaction score, PP: percentage of positive cells)

	Stage (n)	ER α		MTA3		Snail		E-cadherin	
		PP	IRS	PP	IRS	PP	IRS	PP	IRS
UICC	I: 2, II:8, III: 16	0.798	0.608	0.442	0.935	0.769	0.301	0.702	0.800
Lymph node	N(0): 10, N(1): 16	0.901	0.365	0.331	0.722	0.470	0.253	0.529	0.573
Differentiation	M: 14, M to P: 6, P: 6	0.237	0.402	0.583	0.376	0.429	0.232	0.010*	0.018*

3.1.3 Correlation of ER α , MTA3, Snail and E-cadherin in human PDAC

With the presence of ER α , MTA3, Snail and E-cadherin in human PDAC tissues, the connection among these factors was further analyzed *in situ*.

Immunostaining of ER α in cytoplasm correlated with MTA3, Snail and E-cadherin in the area of duct-like structures of human PDAC tissues. In addition, as shown in a series of consecutive sections, a limited number of PDAC cells with nuclear ER α in duct-like structures with nuclear staining of MTA3 had no Snail in the nucleus in conjunction with strong membrane immunoreactions for E-cadherin (Figure 6).

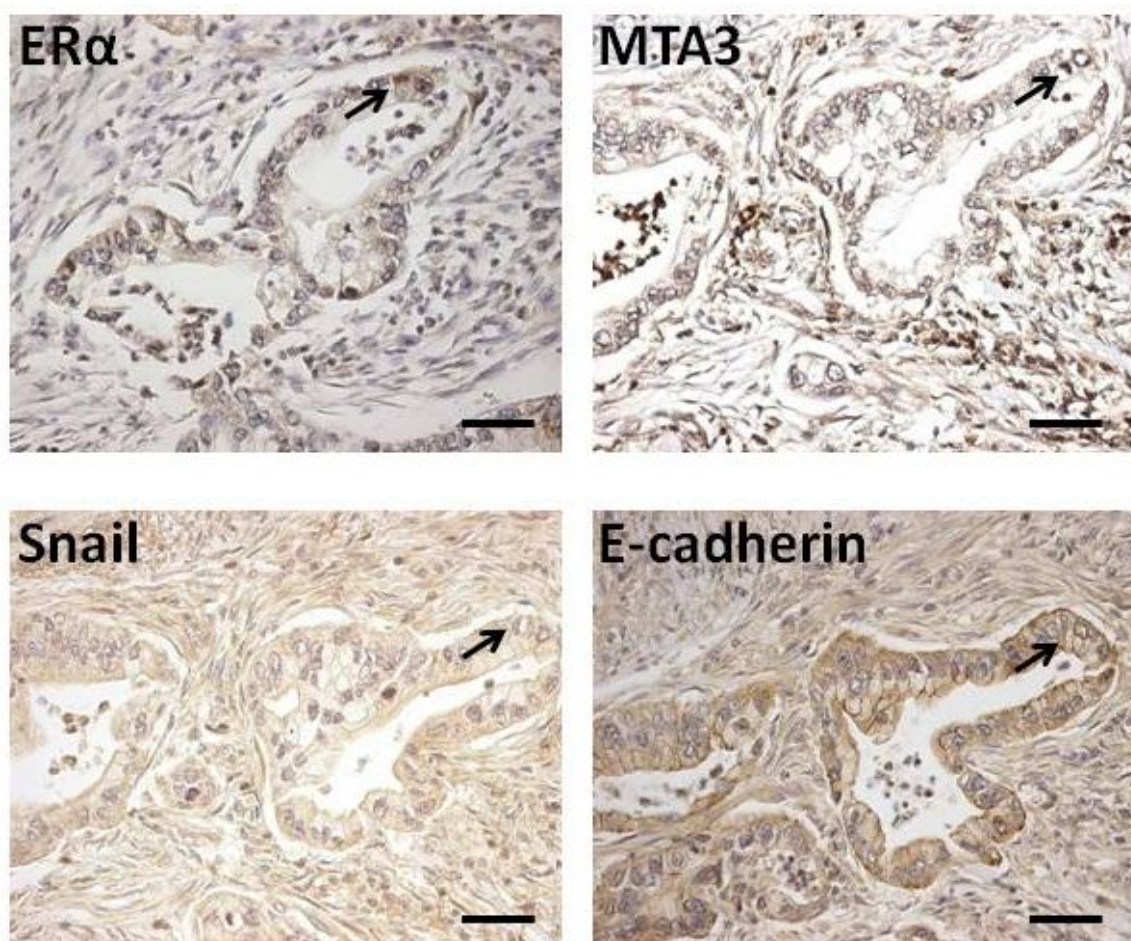


Figure 6: Immunohistochemical staining for ER α , MTA3, Snail and E-cadherin in consecutive sections (3 μ m) from human primary PDAC tissues. Representative images (1/26) for the following staining of FFPE samples with peroxidase-coupled rabbit specific secondary antibodies: ER α by rabbit-derived polyclonal anti-human ER α , MTA3 by rabbit-derived polyclonal anti-human MTA3, Snail by rabbit-derived polyclonal anti-human Snail. E-cadherin by rabbit-derived

polyclonal anti-human E-cadherin. Arrows mark positive cells. (scale bars: 250 μm , original magnification: 400x)

3.1.4 *In-situ* proliferation

To determine the *in-situ* proliferation profile of human PDAC tissues, proliferating cells were detected via PCNA by immunohistochemistry. Nuclear PCNA was found in all examined patients (26/26) (Figure 7). 96% (25/26) of all cases of human PDAC tissues had ER α in cytoplasm and 50% (13/26) of all cases of human PDAC tissues had MTA3 in the nuclei. All human PDAC tissues with positive staining of ER α (25/25) and MTA3 (13/13) were in a proliferating status with nuclear expression of PCNA.

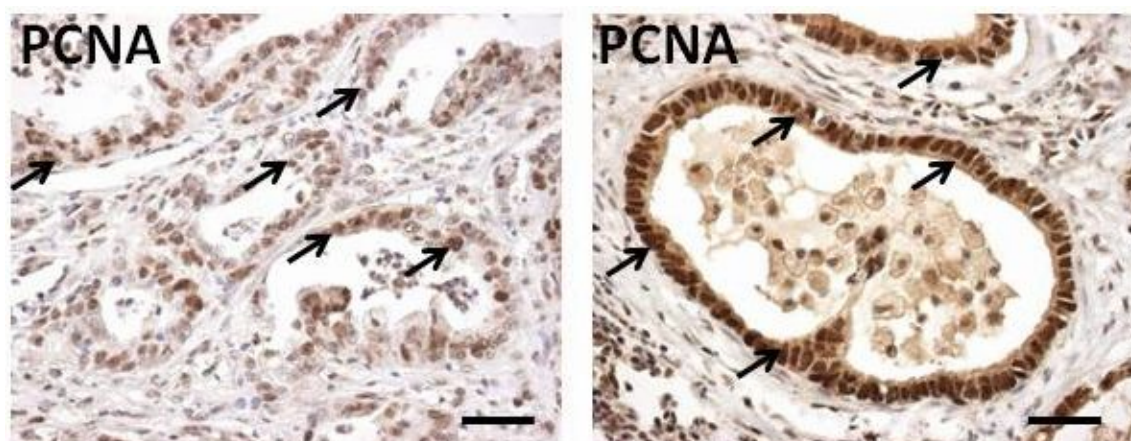


Figure 7: Immunohistochemical staining for PCNA in human primary PDAC tissues. FFPE samples (3 μm) of human PDAC tissue were stained with rabbit-derived polyclonal anti-human PCNA. Primary antibody binding was detected using a peroxidase-coupled rabbit specific secondary antibody. PCNA⁺ cells appear in brown (arrows). Representative images (26/26) showed the moderate (left) and strong (right) immunostaining of PCNA in the nuclei of human PDAC tissues (scale bars: 250 μm , original magnification: 400x)

3.2 Molecules of the ER α signaling pathway in human pancreatic cancer cell lines *in vitro*

3.2.1 Localization by immunocytochemistry/immunofluorescence

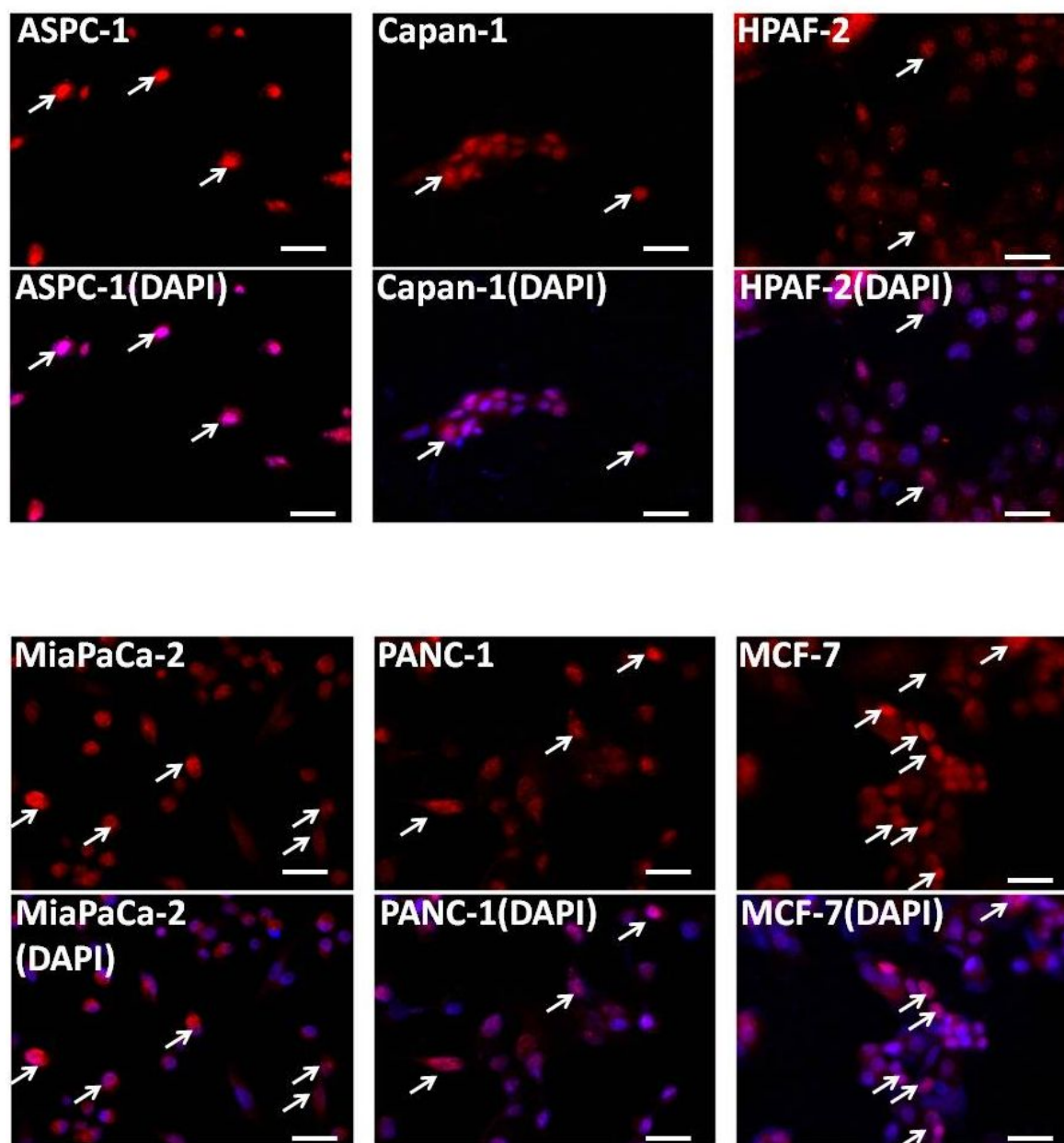
3.2.1.1 ER α

Permanent human pancreatic cancer cell lines derived from a single pancreatic cancer cell are more equal compared to human PDAC tissues composed of a panel of cancer cells. No single pancreatic cell line can represent the variety of human pancreatic cancer, however, some important differences can be detected in these cell lines. The next issue was to determine whether permanent human pancreatic cancer cell lines comprise the molecules of this ER α -governed signaling pathway shown in primary human PDAC tissues.

Immunohistochemistry of ER α was performed in five pancreatic cancer cell lines (ASPC-1, Capan-1, HPAF-2, MiaPaCa-2, and PANC-1) and the breast cancer cell line MCF-7. Although immunostaining was found in the nucleus and cytoplasm of pancreatic cancer cell lines, nuclear signals were too weak to be easily distinguished from the hematoxylin counterstaining (not shown).

Thus immunofluorescence staining was carried out and nuclear ER α was confirmed in all 5 pancreatic cancer cell lines as well as in the MCF-7 cell line which was used as a positive control (Figure 6). About 70% of MCF-7 cells had a strong ER α expression in the nucleus, whereas the signal in human pancreatic cancer cell lines was of lower intensity. Moderate immunostaining was observed in the nuclei of 60% of MiaPaCa-2 cells which were more frequent than those observed in PANC-1 and ASPC-1 (40%), while the more differentiated Capan-1 and HPAF-2 cell lines had only about 20% positive nuclear staining for ER α (Figure 8B).

A



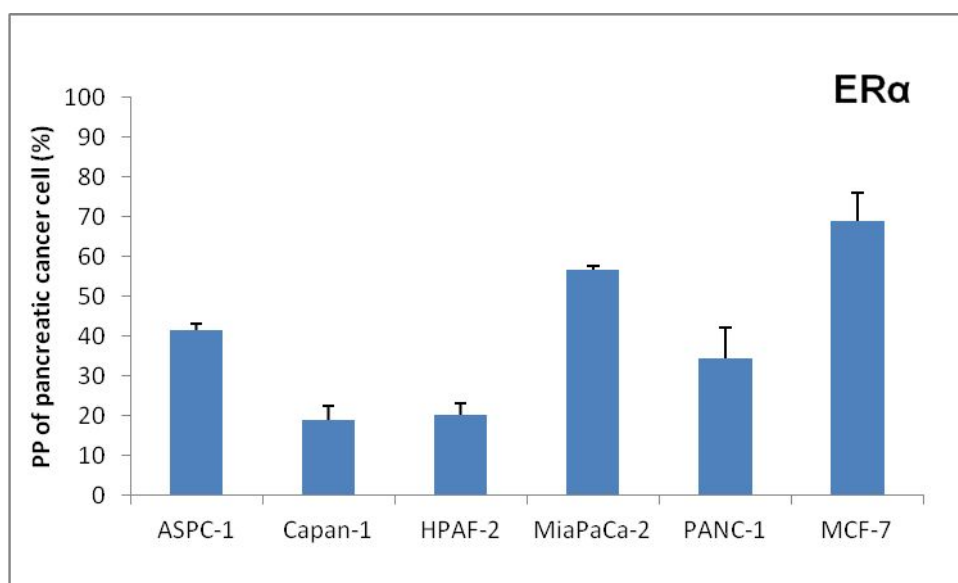
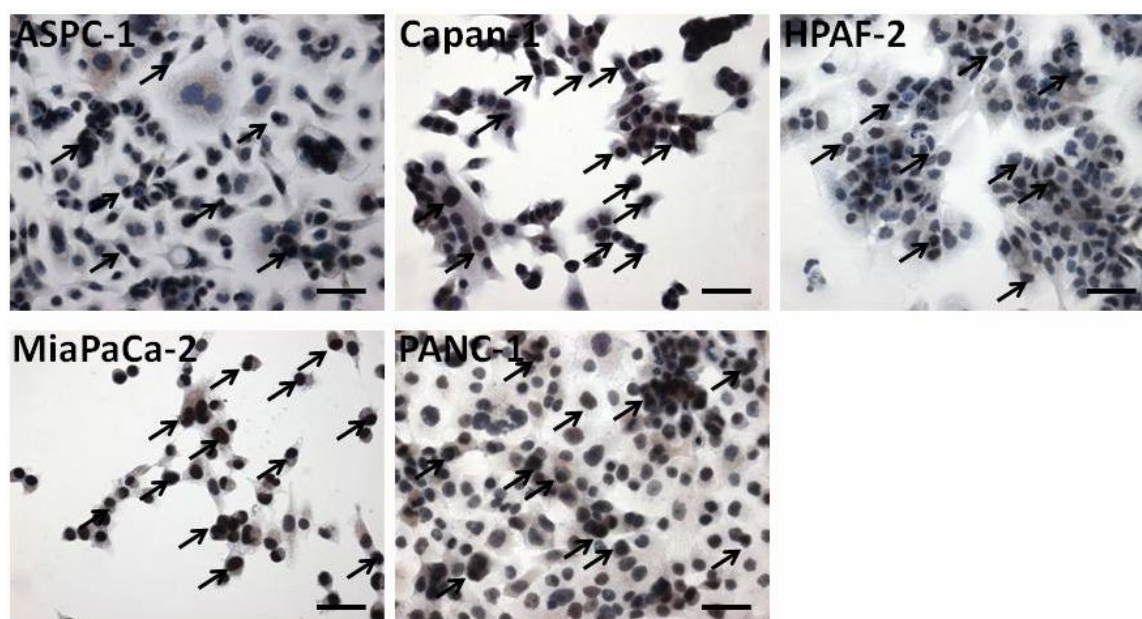
B

Figure 8: (A) Immunofluorescence staining for ER α in human pancreatic cancer cell lines. ASPC-1, Capan-1, HPAF-2, MiaPaCa-2, and PANC-1 cells as well as the human breast cancer cell line MCF-7 as control grown on glass slides were stained with rabbit-derived polyclonal anti-human ER α . Primary antibody binding was detected using a Texas-Red-conjugated rabbit specific secondary antibody and counterstained with DAPI. ER α ⁺ cells appear in red (arrows), nuclei appear in blue. Representative images for nuclear localization of ER α in the cell lines as indicated. (scale bars: 250 μ m, original magnification: 400x) (B) Mean values \pm SD of the proportion of ER α ⁺ cells from 3 HPF of 3 individual slides. (PP: percentage of positive cells)

3.2.1.2 MTA3

MTA3, a downstream molecule of ER α signaling, was analyzed in pancreatic cancer cell lines (Figure 9). Specific immunoreactions for MTA3 were found in all five human pancreatic cancer cell lines, more strongly in the nucleus and more weakly in the cytoplasm (Figure 9A). About 80% of MiaPaCa-2 and Capan-1 cells had nuclear MTA3 followed by PANC-1 cells (60%), HPAF-2 and ASPC-1 cells (40%) (Figure 9B).

A



B

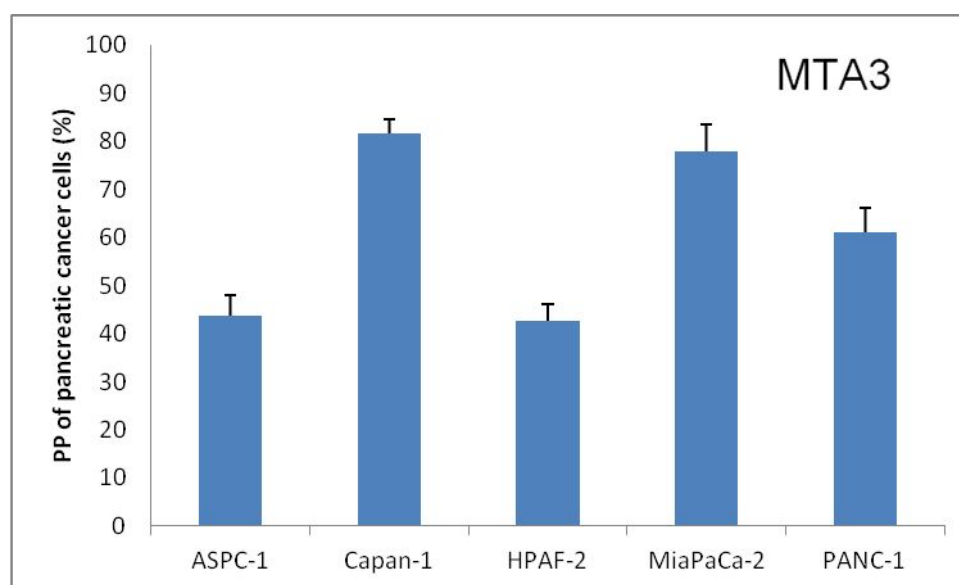
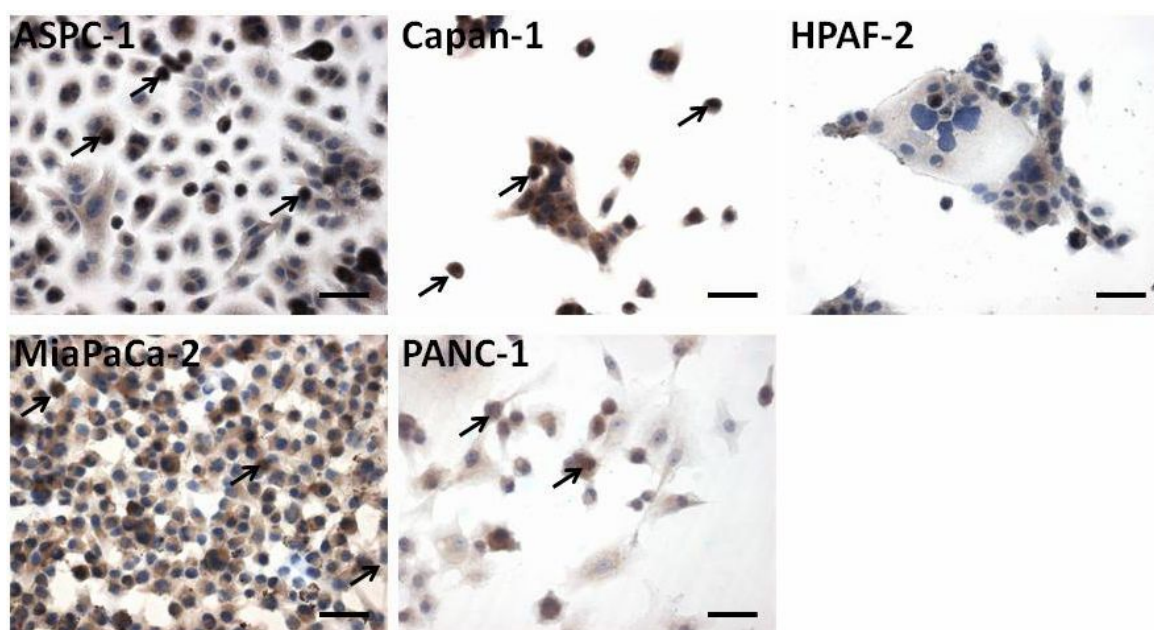


Figure 9: (A) Immunocytochemical staining for MTA3 in human pancreatic cancer cells. ASPC-1, Capan-1, HPAF-2, MiaPaCa-2 and PANC-1 grown on glass slides were stained with rabbit-derived polyclonal anti-human MTA3. Primary antibody binding was detected using a peroxidase-coupled rabbit-specific secondary antibody, developed with DAB and counterstained with hematoxylin. MTA3⁺ cells appeared in brown staining in the nucleus (arrows). Representative images for nuclear localization of MTA3 in the cell lines as indicated. (scale bars: 250 μ m, original magnification: 400x) (B) Mean values \pm SD of the proportion of MTA3⁺ cells from 3 HPF of 3 individual slides. (PP: percentage of positive cells)

3.2.1.3 Snail

ER α and MTA3 act on downstream targets like Snail and E-cadherin. The transcription factor Snail and the adhesion molecule E-cadherin are widely accepted as core regulators of EMT. The next experiment was done to investigate Snail and E-cadherin in human pancreatic cancer cell lines. Snail was detected in 4 of 5 pancreatic cancer cell lines with a moderate nuclear staining (Figure 10A). Whereas Capan-1 cells had nuclear immunoreactions in 20% of cells compared to 15% in PANC-1 cells, 10% in MiaPaCa-2 and 5% in ASPC-1 cells, no signal was found in the HPAF-2 cell line (Figure 10B).

A



B

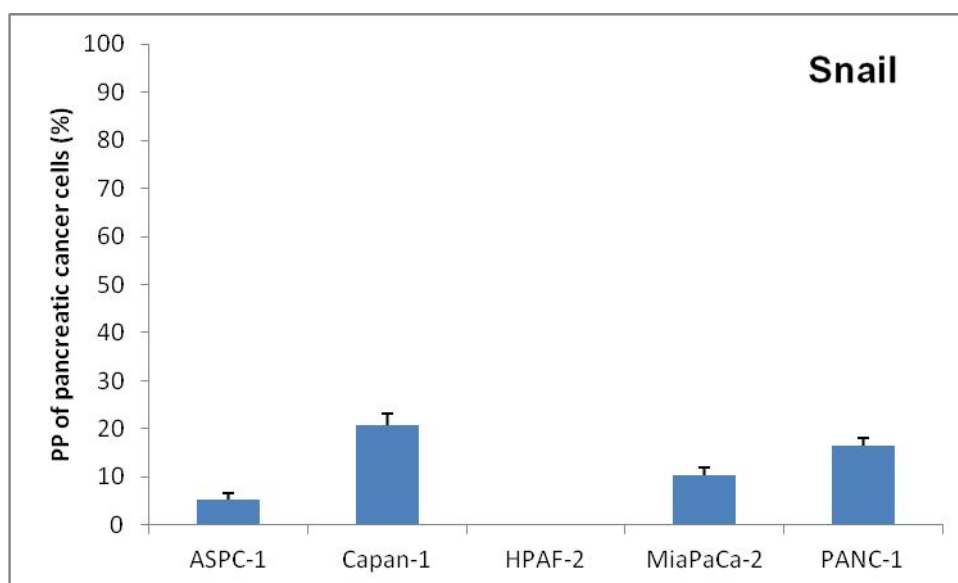


Figure 10: (A) Immunocytochemical staining for Snail in human pancreatic cancer cells. ASPC-1, Capan-1, HPAF-2, MiaPaCa-2, and PANC-1 cell lines grown on glass slides were stained with rabbit-derived polyclonal anti-human Snail. Primary antibody binding was detected using a peroxidase-coupled rabbit-specific secondary antibody, developed with DAB and counterstained with hematoxylin. Nuclei of Snail⁺ cells appeared in brown (arrows). Some HPAF-2 cells appeared to be positive because they are not at the same level with other cells. With a different focal length, the blue staining in the nuclei can be clearly identified. However, this cannot be demonstrated here, since the other cells would appear to have a positive staining. Representative images are shown for nuclear localization of Snail in cell lines as indicated. (scale bars: 250 μ m, original magnification: 400x) (B) Mean values \pm SD of the proportion of MTA3⁺ cells from 3 HPF of 3 individual slides. (PP: percentage of positive cells)

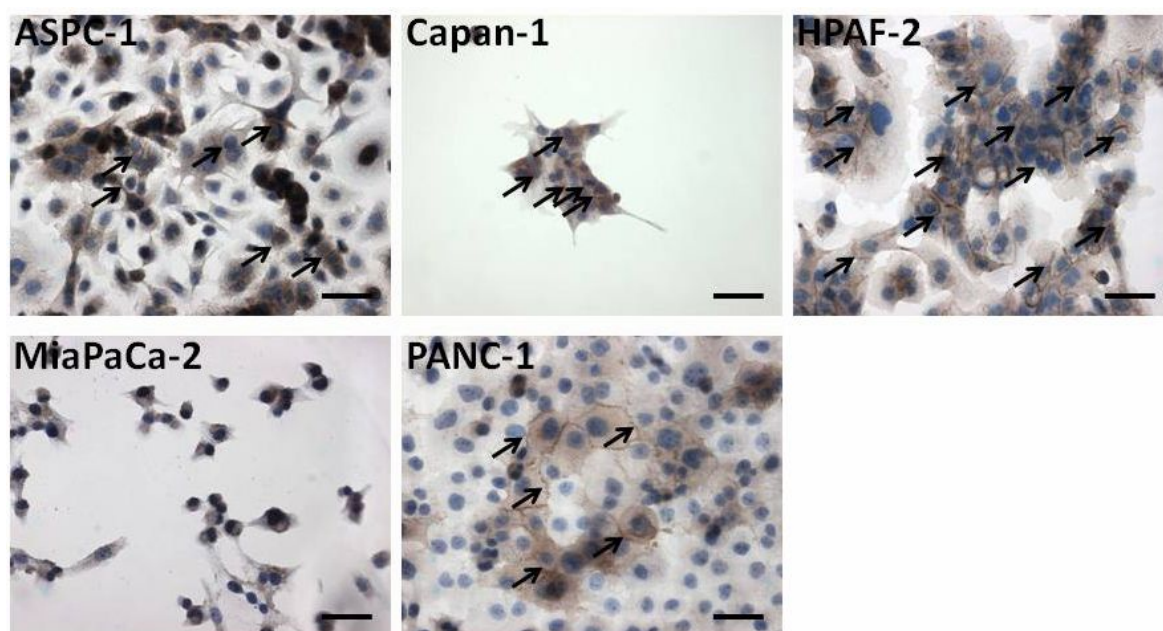
3.2.1.4 E-cadherin

E-cadherin in human pancreatic cancer cell lines was assessed by immunocytochemistry and detected in 4 of the 5 cell lines with a brown staining of intercellular borders. In HPAF-2 cells, 80% of the cells had strong membrane staining followed by Capan-1 cells (50%). ASPC-1 and PANC-1 cells showed a moderate expression in about 30% and 20% of the cancer cells, while the undifferentiated MiaPaCa-2 cell line exhibited no E-cadherin expression.

In conclusion, ER α and its downstream molecules MTA3, Snail and E-cadherin detected in the human pancreatic cancer cell lines HPAF-2, Capan-1, ASPC-1,

PANC-1 and MiaPaCa-2 represent different levels of metastatic potential.

A



B

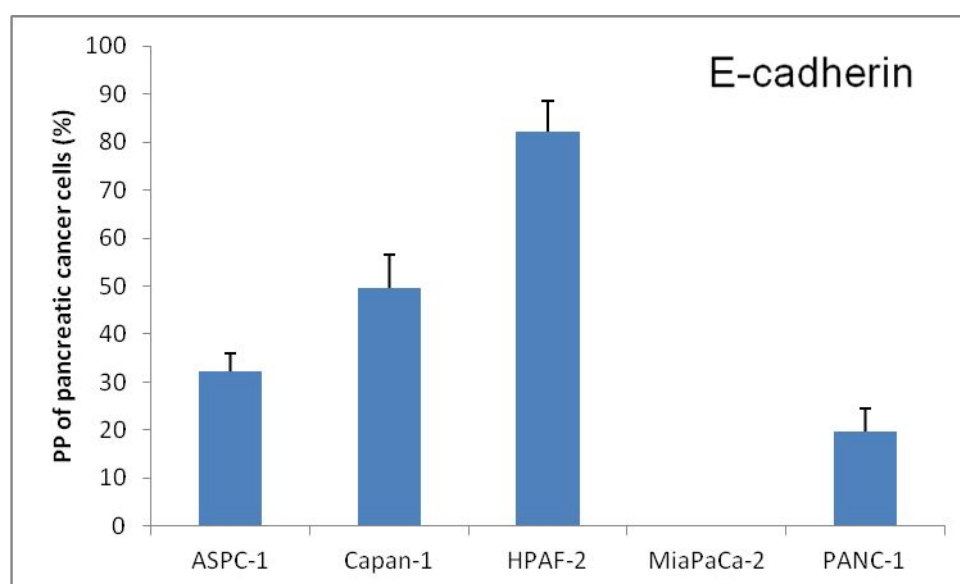


Figure 11: (A) Immunocytochemical staining for E-cadherin in human pancreatic cancer cells. ASPC-1, Capan-1, HPAF-2, MiaPaCa-2 or PANC-1 grown on glass slides were stained with rabbit-derived polyclonal anti-human E-cadherin. Primary antibody binding was detected using a peroxidase-coupled rabbit specific secondary antibody, developed with DAB and counterstained with hematoxylin. E-cadherin+ cells appeared in brown staining in the membrane (arrows). Representative images for nuclear localization of E-cadherin in the cell lines as indicated. (scale bars: 250 μ m, original magnification: 400x) (B) Mean values \pm SD of the proportion of

E-cadherin⁺ cells from 3 HPF of 3 individual slides. (PP: percentage of positive cells)

3.2.2 Expression of ER α , MTA3, Snail, and E-cadherin at mRNA level of pancreatic cancer cell lines

Semi-quantitative RT-PCR was used to identify the ER α -related signaling molecules shown above at the mRNA level. Again, the human breast cancer cell MCF-7 was used as control to estimate the expression levels in the human pancreatic cancer cell lines ASPC-1, Capan-1, HPAF-2, MiaPaCa-2 and PANC-1 (Figure 12).

ER α -mRNA was identified with different intensities in all pancreatic cancer cell lines. The poorly differentiated PANC-1 cell line had a strong expression followed by HPAF-2 with expression levels comparable to MCF-7 cells. MiaPaCa-2 ASPC-1 and Capan-1 cells displayed weaker expression signals.

MTA3-mRNA was found in all pancreatic cancer cell lines. The cell lines ASPC-1, Capan-1, and PANC-1 showed a strong expression comparable to the MCF-7 cell line used as positive control. Expression levels in HPAF-2 and MiaPaCa-2 cells were only slightly lower than those found in the other cell lines.

Snail-mRNA was detected in all five pancreatic cancer cell lines as well as in the MCF-7 cell line with the strongest signal in the poorly differentiated PANC-1 cells followed by the undifferentiated MiaPaCa-2 cell line and poorly differentiated ASPC-1 cell line in the range of MCF-7 cells. Well differentiated Capan-1 and moderately differentiated HPAF-2 cells showed the lowest Snail expression.

E-cadherin-mRNA was found in four of five pancreatic cancer cell lines as well as in the MCF-7 cell line. The undifferentiated human pancreatic cancer cell line MiaPaCa-2 revealed no expression of E-cadherin.

These results indicated at the mRNA level that except for MiaPaCa-2 cells, all pancreatic cancer cell lines tested expressed ER α and the main down-stream molecules of this EMT-related signaling pathway. Therefore these cell lines were assumed to be good models for studying ER α -dependent mechanisms in human PDAC.

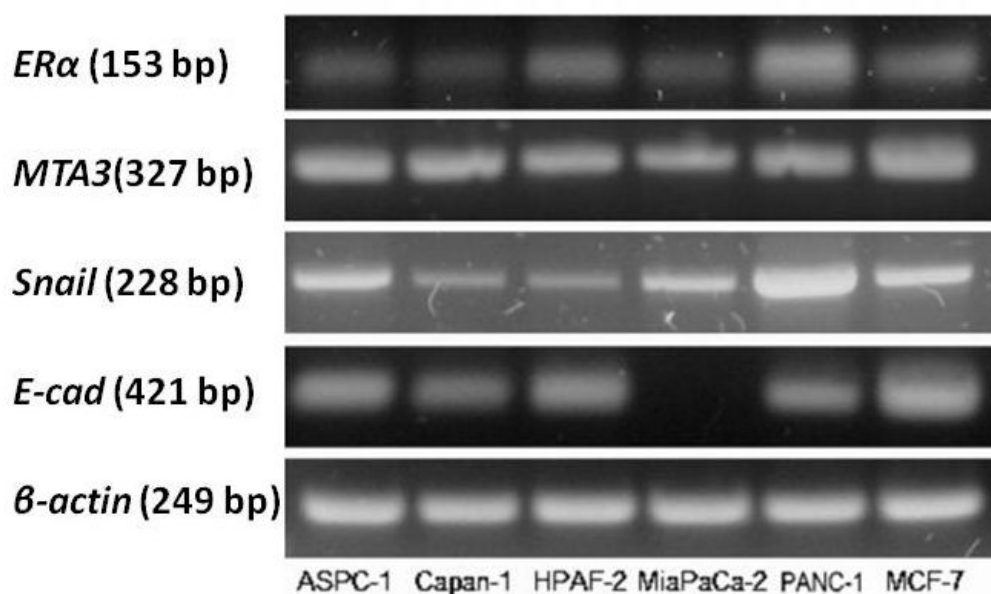


Figure 12: Semi-quantitative assessment of ER α , MTA3, Snail and E-cadherin in human pancreatic and breast cancer cell lines at the mRNA level. ASPC-1, Capan-1, HPAF-2, MiaPaCa-2, PANC-1 and MCF-7 cells were lysed and 2 μ g of the total cellular RNA were reversely transcribed. First-strand cDNA was amplified with transcript-specific oligonucleotides for ER α , Snail, MTA3, and E-cadherin (E-cad). β -actin was used to verify integrity and amount of RNA. All PCR products separated by agarose gel electrophoresis were visualized under UV light. Representative images of at least 3 independent experiments with triplicate determinations.

3.2.3 Overall expression at the protein level

To strengthen the results from immunohistochemistry and from the transcriptional level, expression of these molecules in human pancreatic cancer cell lines was further checked by Western blot analysis (Figure 13).

In contrast to immunofluorescence data, no ER α protein was detected in all pancreatic cancer cell lines, while the MCF-7 cell line used for positive control displayed a strong specific signal for ER α .

MTA3 signals were generally weak, MiaPaCa-2, and PANC-1 cell lines showed even weaker signal intensity.

Snail was found in 4 of 5 pancreatic cancer cell lines as well as in MCF-7 cells. The most undifferentiated human pancreatic cancer cell line MiaPaCa-2 and the well differentiated Capan-1 cells had the strongest expression. Low and very low

expression was observed for PANC-1 and HPAF-2 cells. ASPC-1 did not express Snail.

A strong E-cadherin band intensity comparable to that of the MCF-7 cell line was detected in the well to moderately differentiated human pancreatic cancer cell lines Capan-1 and HPAF-2, while no expression was found in undifferentiated MiaPaCa-2 or poorly differentiated PANC-1 cell lines.

Expression of MTA3, Snail and E-cadherin as shown in Western blot analysis was consistent with the findings by immunocytochemistry while no ER α was detected. Comparable to immunocytochemistry, RT-PCR and western blot data from human pancreatic cancer cells, the expression of ER α and its related elements in governing EMT (MTA3, Snail and E-cadherin) were detected in the Capan-1 cell line.

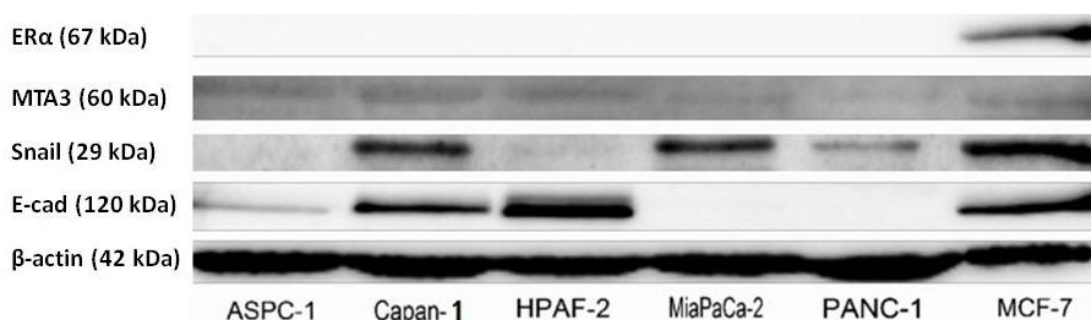


Figure 13: Western blot analysis for ER α , MTA3, Snail and E-cadherin in human pancreatic and breast cancer cells. ASPC-1, Capan-1, HPAF-2, MiaPaCa-2, PANC-1 and MCF-7 cells were lysed. Total protein extracts (50 μ g) separated by SDS-PAGE were exposed to rabbit-derived polyclonal anti-human ER α , MTA3, Snail, E-cadherin (E-cad) and β -actin. Primary antibody binding was detected using a peroxidase-coupled rabbit specific secondary antibody and luminescence imaging. β -actin was used to verify integrity and amount of protein. Representative images of at least 3 independent experiments with triplicate determinations. Sizes of the individual transcripts are indicated.

3.3 Localization of molecules of the ER α signaling pathway and proliferation within orthotopic xenografts of human pancreatic cancer cell lines in nude mice *in situ*

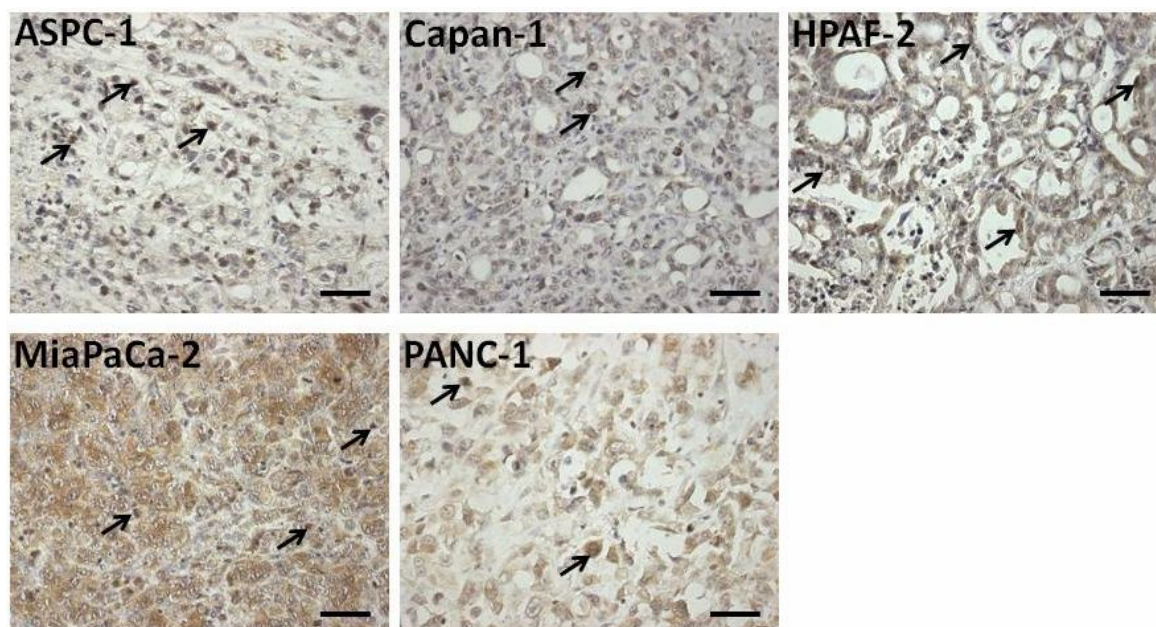
3.3.1 ER α

Expression of ER α and the downstream molecules MTA3, Snail and E-cadherin was

confirmed in human primary PDAC tissues and human pancreatic cancer cell lines. The final experiments focused on the expression of these molecules in orthotopic nude mice xenografts. The orthotopic xenografts provide the *in vivo* information about the tumor formation and progression from different pancreatic cell lines.

Nuclear and cytoplasmic immunostaining of ER α was found *in situ* in the orthotopic tumors of all 5 human pancreatic cancer cell lines. ER α was found more often in the cytoplasm of duct-like pancreatic cancer cells. The intensities and frequency were calculated by light microscopy. HPAF-2 cells had about 40% of cancer cells with moderate ER α staining followed by MiaPaCa-2 (30%) and ASPC-1 (30%). Capan-1 and PANC-1 had only 10% of cancer cells that disclosed weak ER α expression.

A



B

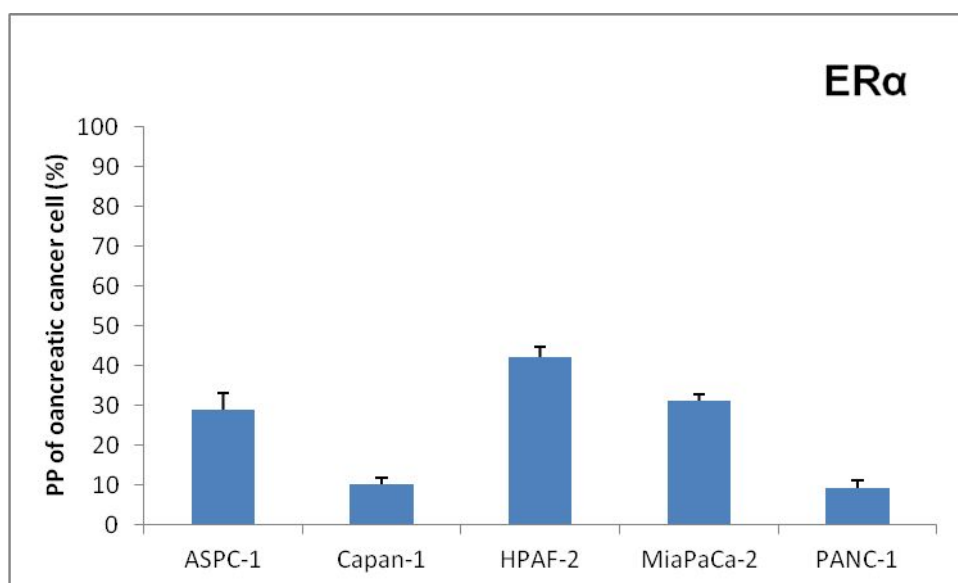


Figure 14: (A) Immunohistochemical staining for ER α in human pancreatic cancer xenografts in nude mice. Formalin-fixed paraffin-embedded (FFPE) samples (3 μ m) of human pancreatic cancer xenografts in nude mice were stained with rabbit-derived polyclonal anti-human ER α . Primary antibody binding was detected using a peroxidase-coupled rabbit specific secondary antibody, developed with DAB, and counterstained with hematoxylin. ER α ⁺ cells appeared in brown staining in the nucleus (arrows). Representative images showed nuclear and cytoplasmic localization of ER α in ASPC-1, Capan-1, HPAF-2, MiaPaCa-2, and PANC-1. (scale bars: 250 μ m, original magnification: 400x) (B) Mean values \pm SD of the proportion of ER α ⁺ cells from 3 HPF of 3 individual slides. (PP: percentage of positive stained cells)

3.3.2 MTA3

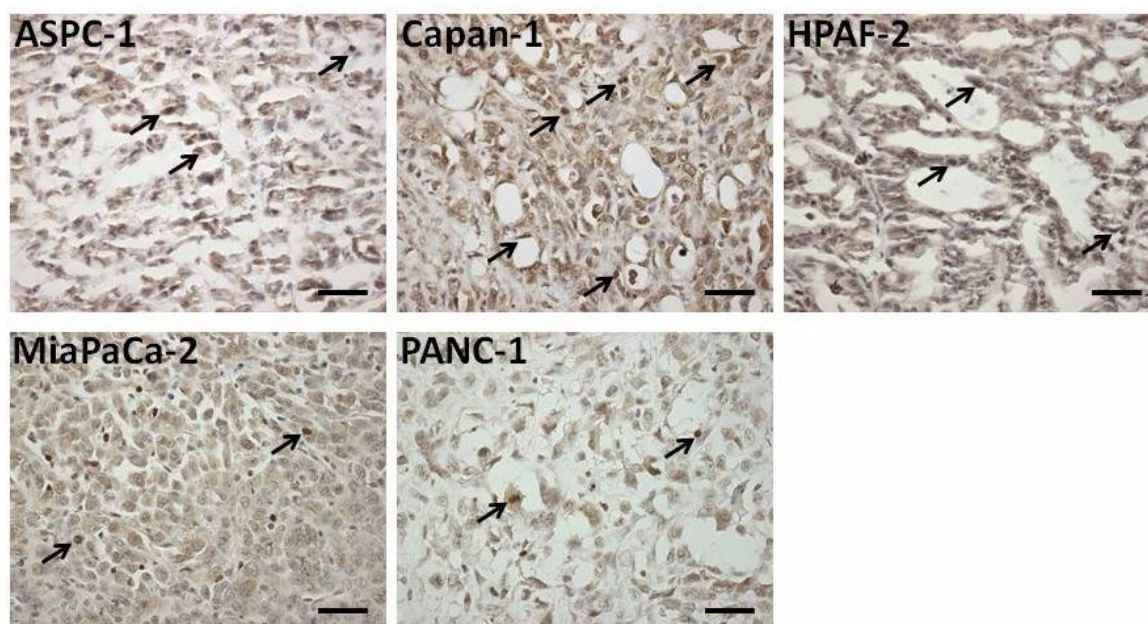
Immunohistochemistry was performed to detect MTA3 expression in orthotopic nude mice xenografts (Figure 15).

MTA3 was found in the human pancreatic cancer cell lines with nuclear and cytoplasmic immunoreactions (Figure 15A). MTA3 was located in the pancreatic cancer cells in well differentiated duct-like structures where cytoplasmic staining of ER α was also found. In better differentiated cell lines like ASPC-1, MTA3 expression was frequently seen in Capan-1 and HPAF-2, which had duct-like structures in cancer tissues.

The proportion of MTA3⁺ cells within the tumors derived from human pancreatic

cancer cell lines was estimated (Figure 15B). Within the tumors derived from Capan-1 cells, 50% of the pancreatic cancer cells had a strong signal followed by those derived from ASPC-1 and HPAF-2 cell lines. Transferring MiaPaCa-2 or PANC-1 cells led to only about 10% of pancreatic cancer cells with strong nuclear staining of MTA3.

A



B

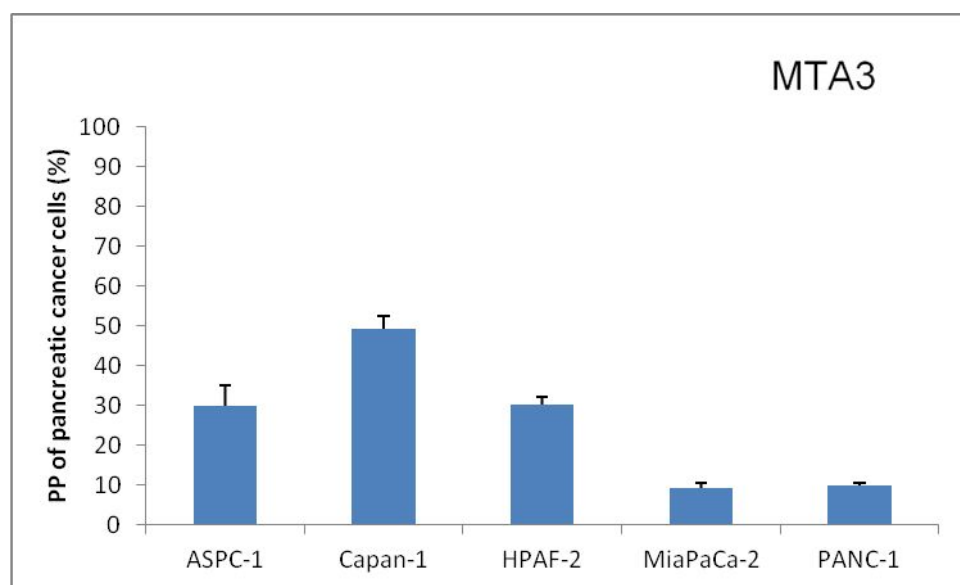


Figure 15: (A) Immunohistochemical staining for MTA3 in human pancreatic cancer xenografts in nude mice. Formalin-fixed paraffin-embedded (FFPE) samples (3 μ m) of human pancreatic cancer xenografts in nude mice were stained with rabbit-derived polyclonal anti-human MTA3. Primary antibody binding was detected using a peroxidase-coupled rabbit specific secondary antibody, developed with DAB, and counterstained with hematoxylin. MTA3⁺ cells appeared in brown staining in the nucleus (arrows). Representative images showed nuclear and cytoplasmic localization of MTA3 in ASPC-1, Capan-1, HPAF-2, MiaPaCa-2, and PANC-1. (scale bars: 250 μ m, original magnification: 400x) (B) Mean values \pm SD of the proportion of MTA3⁺ cells from 3 HPF of 3 individual slides. (PP: percentage of positive stained cells)

3.3.3 Snail

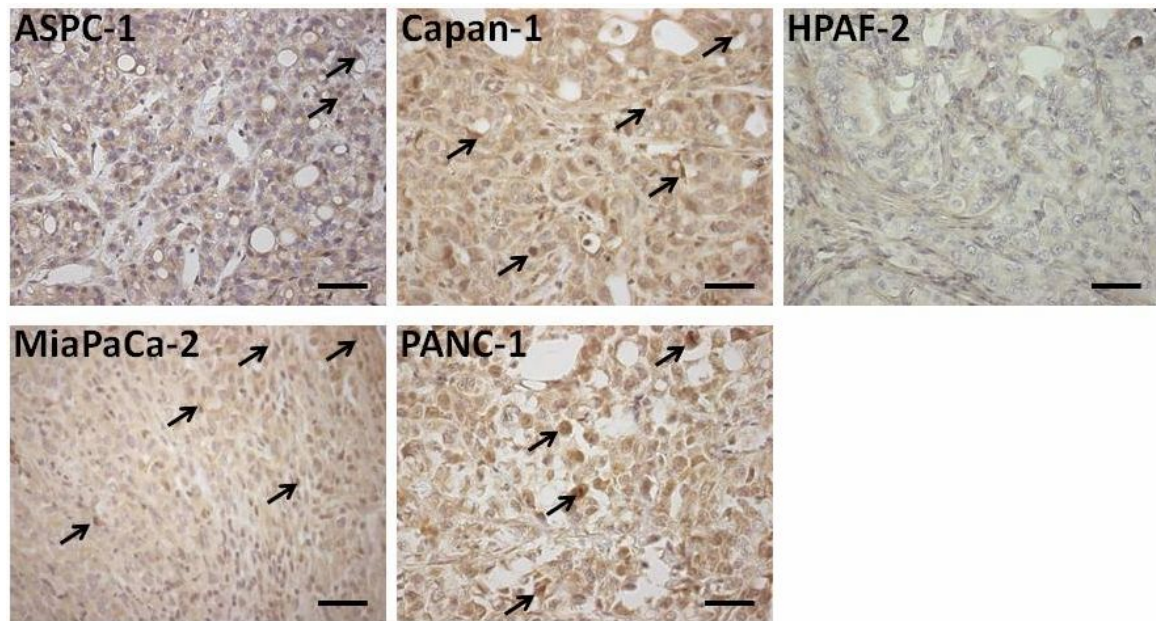
Further investigations were focused on the localization of Snail expression in orthotopic nude mice xenografts (Figure 16).

Nuclear and cytoplasm staining of Snail was found in tumors after transferring each of the 5 human pancreatic cancer cell lines into nude mice (Figure 16A). In tissues from the group that received Capan-1 or ASPC-1, strong Snail staining was found in the pancreatic cancer cells from duct-like structures. Consequently, the undifferentiated pancreatic cancer cell line MiaPaCa-2 did not develop duct-like structures within the murine model.

The proportions of pancreatic cancer cells with positive Snail staining were calculated

in the tumors deriving from each individual human pancreatic cancer cell line. The undifferentiated MiaPaCa-2 cell line gave rise to about 40% Snail⁺ cells with strong staining followed by Capan-1 and PANC-1 (30%; Figure 16B). The moderately differentiated HPAF-2 cell line did not result in nuclear Snail staining.

A



B

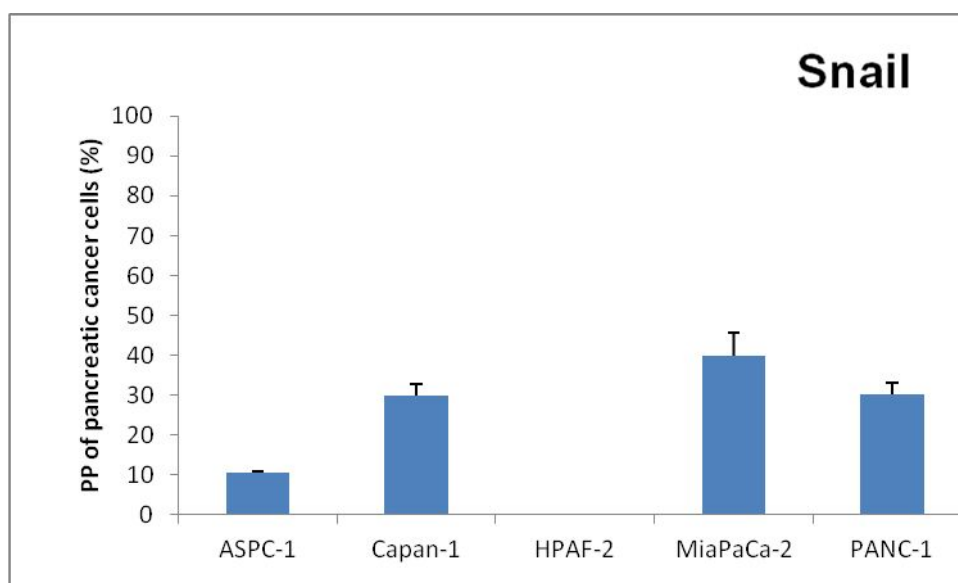


Figure 16: (A) Immunohistochemical staining for Snail in human pancreatic cancer xenografts in nude mice. Formalin-fixed paraffin-embedded (FFPE) samples (3 μm) of human pancreatic cancer xenografts in nude mice were stained with rabbit-derived polyclonal anti-human Snail. Primary antibody binding was detected using a peroxidase-coupled rabbit specific secondary antibody, developed with DAB, and counterstained with hematoxylin. Snail⁺ cells appeared in brown staining in the nucleus (arrows). Representative images shows nuclear localization of Snail in ASPC-1, Capan-1, HPAF-2, MiaPaCa-2, and PANC-1 cells. (scale bars: 250 μm , original magnification: 400x) **(B)** Mean values \pm SD of the proportion of Snail⁺ cells as from 3 HPF of 3 individual slides. (PP: percentage of positive stained cells)

3.3.4 E-cadherin

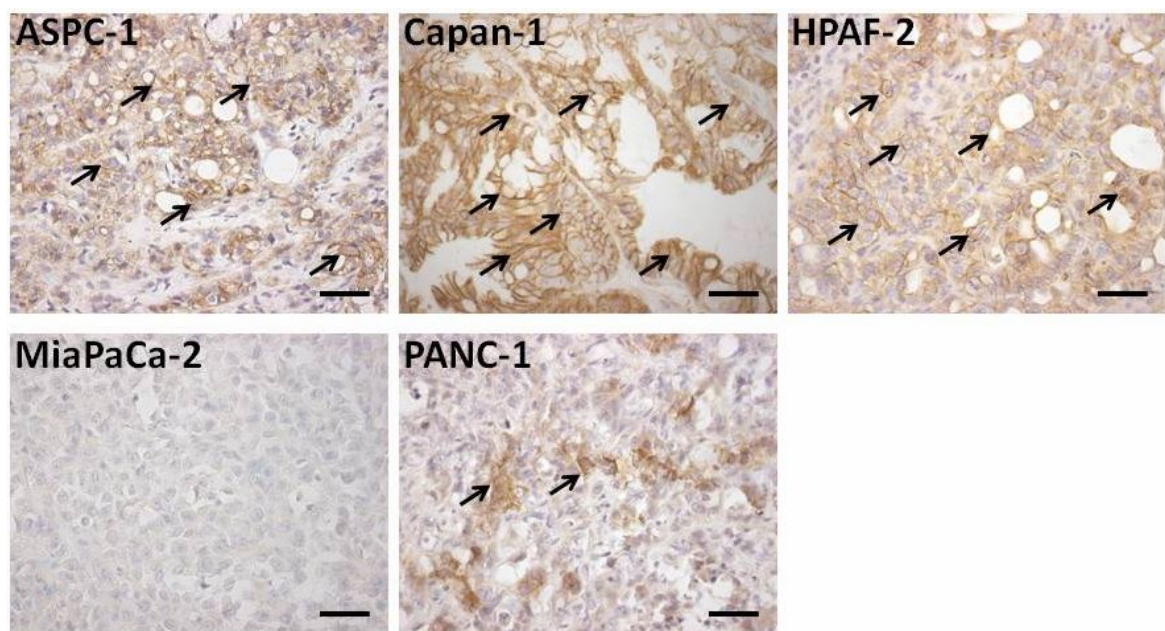
E-cadherin was detected in the membranes of human pancreatic cancer cells from orthotopic nude mice xenografts with a brown staining (Figure 17A).

This was mainly observed in the duct-like pancreatic cancer cells obtained from the moderately differentiated Capan-1 and HPAF-2 cell lines with about 70-80% strong E-cadherin⁺ pancreatic cancer cells (Figure 17B). ASPC-1 gave rise to about 50% of pancreatic cancer cells with moderate E-cadherin staining followed by PANC-1 with about 10% of pancreatic cancer cells with moderate E-cadherin staining. Again, the absence of duct-like structures inside the tumors from the undifferentiated human pancreatic cancer cell line MiaPaCa-2 was accompanied by the absence of

E-cadherin.

These findings in orthotopic nude mice xenografts of the human pancreatic cancer cell lines that were also shown to express mainly molecules of the ER α -related signaling pathway *in vitro* confirmed the findings obtained in human PDAC tissues. It further suggested that these molecules might be necessary for tumor growth/development from human pancreatic cancer cells.

A



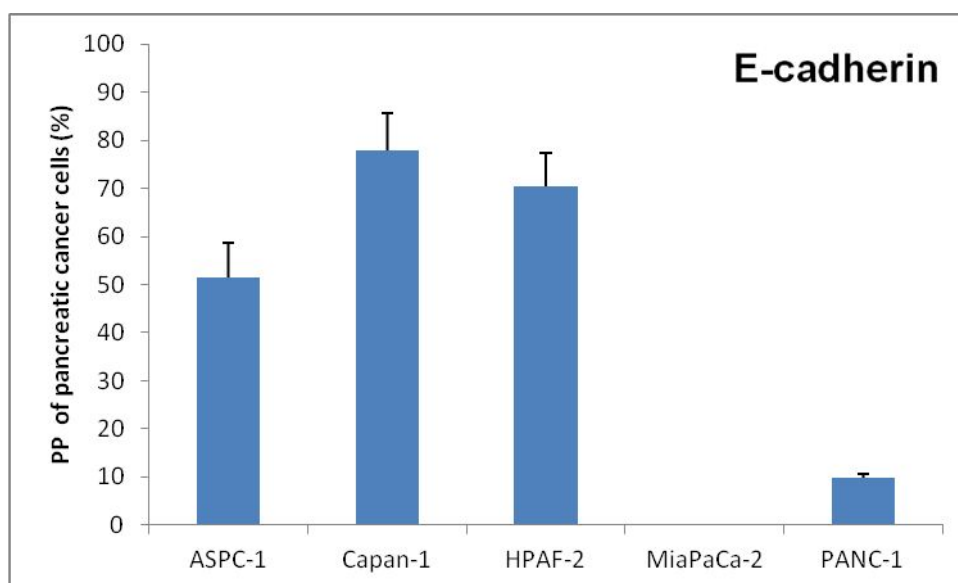
B

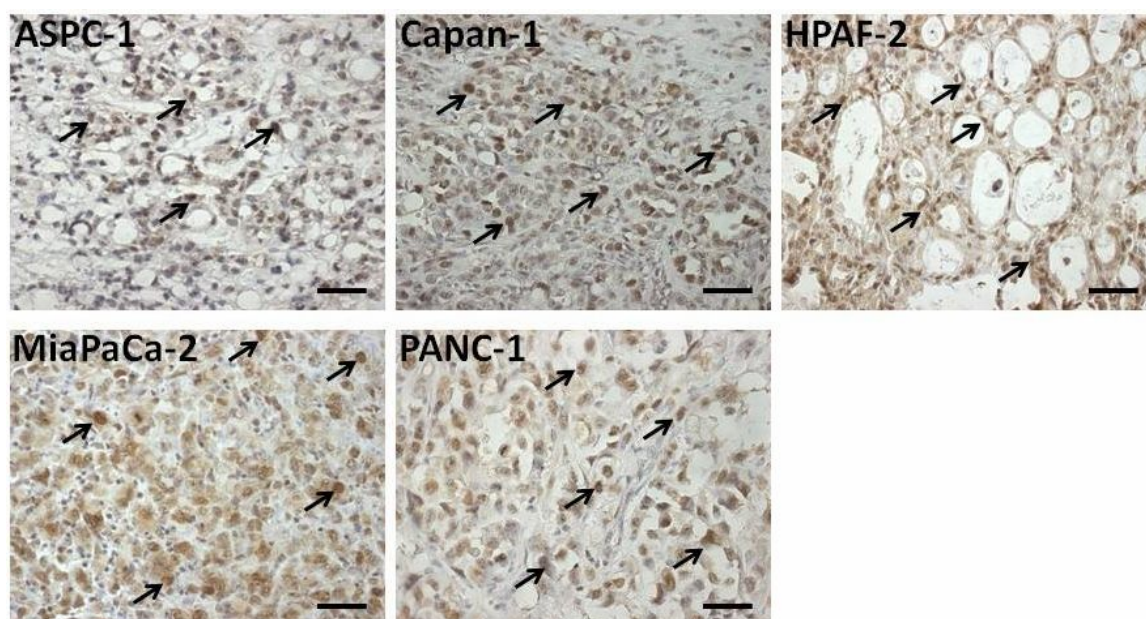
Figure 17: (A) Immunohistochemical staining for E-cadherin in human pancreatic cancer xenografts in nude mice. Formalin-fixed paraffin-embedded (FFPE) samples (3 μm) of human pancreatic cancer xenografts in nude mice were stained with rabbit-derived polyclonal anti-human E-cadherin. Primary antibody binding was detected using a peroxidase-coupled rabbit specific secondary antibody, developed with DAB, and counterstained with hematoxylin. E-cadherin⁺ cells appeared in brown staining in the membrane (arrows). Representative images shows membrane localization of E-cadherin in ASPC-1, Capan-1, HPAF-2, MiaPaCa-2, and PANC-1. (scale bars: 250 μm , original magnification: 400x) (B) Mean values \pm SD of the proportion of E-cadherin⁺ cells from 3 HPF of 3 individual slides. (PP: percentage of positive stained cells)

3.3.5 *In-situ* proliferation

Proliferation of cells from the human pancreatic cancer cell lines in nude mouse xenografts was determined by immunohistochemistry for PCNA (Figure 18A).

PCNA was found in tissues derived from all five human cell lines with strong nuclear immunoreactions. All five human cell lines give rise to about 90% of PCNA⁺ pancreatic cancer cells (Figure 18B).

A



B

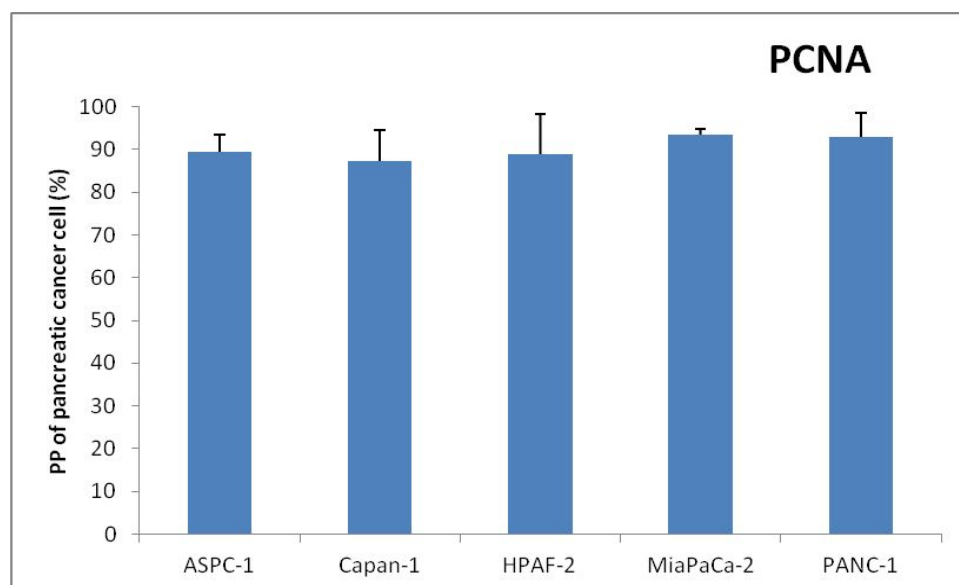


Figure 18: (A) Proliferating human pancreatic cancer cells in human pancreatic cancer xenografts in nude mice were stained with PCNA. Primary antibody binding was detected using a peroxidase-coupled rabbit-specific secondary antibody, developed with DAB, and counterstained with hematoxylin. Snail⁺ cells appeared in brown staining in the nucleus (arrows). PCNA⁺ cells appeared in brown staining in nucleus (arrows). Representative images were for nuclear localization of PCNA in ASPC-1, Capan-1, HPAF-2, MiaPaCa-2 and PANC-1. (scale bars: 250 μ m, original magnification: 400x). (B) Mean values \pm SD of the proportion of Snail⁺ cells from 3 HPF of 3 individual slides. (PP: percentage of positive stained cells)

4 Discussion

4.1 Background

The notion that estrogen plays a role in pancreatic cancer progression was supported by a number of clinical studies, which showed that exposure to estrogen during the reproductive years reduced the risk of pancreatic cancer in women [45, 61]. Several experiments were performed to demonstrate the expression pattern of ER α in human PDAC tissues. However, conflicting findings published in the literature in the last decades suggested that pancreatic cancer cells expressed ER α [38, 62, 63], while other authors detected no ER α in pancreatic cancer [64, 65]. No definite explanation has been found for this discrepancy.

ER α is believed to be a key regulator in breast cancer progression. Fujita et al. demonstrated an important role of ER α in governing the progression of breast cancer via EMT repression, which was widely accepted as the onset of and critical in carcinogenesis and cancer metastasis via the ER α /MTA3/Snail/E-cadherin pathway [35]. ER α activated MTA3 in the presence of estrogen. MTA3 is dedicated to Snail gene repression via histone deacetylase and ATP-dependent chromatin remodeling functions. Thus MTA3 constitutes a component in this signal pathway and connects ER α action by repressing Snail expression. Finally, this ER α -related signaling pathway is manifested in the expression of E-cadherin and the maintenance of a normal epithelial architecture [35]. To address this EMT-related signaling pathway in regulating the progression in pancreatic cancer cells, further knowledge of the expression patterns of ER α and its related receptors MTA3, Snail, E-cadherin is required. The aim of this study was to investigate the expression pattern of ER α and its related elements involved in this EMT-related signaling pathway in human pancreatic cancer.

4.2 Human tissues

Firstly, the expression of ER α , MTA3, Snail, E-cadherin and PCNA was investigated in clinical samples via immunohistochemistry. ER α was detected in human PDAC

tissues as well as in noncancerous pancreas tissues. In cancerous tissues, ER α was mainly found in the cytoplasm and to a lesser extent in the nucleus (Figure 4). However, the intensity and localization of ER α in human PDAC tissues did not depend on the patient's clinical and pathological data: ER α was mainly observed in the cytoplasm of well differentiated duct-like cancerous cells. This observation was consistent with the findings from other groups that ER α is present in human PDAC tissues [64].

MTA3 constitutes a key component in this signaling pathway. In breast cancer cells, MTA3 up-regulated by ER α links the expression of ER α to E-cadherin expression and thus to EMT and cancer progression [57]. However, the expression pattern of MTA3 in pancreatic cancer remains unknown. In this study, MTA3 was found in the nucleus as well as in the cytoplasm of human PDAC tissues (Figure 5). More patients with moderately differentiated PDAC were found to be positive for MTA3 (64%) than those with moderately to poorly and poorly differentiated PDAC (33%). Expression of MTA3 in lymph node-negative patients (60%) was higher than that found in lymph node-positive patients (44%). This observation indicates that MTA3 exists in human PDAC tissues and tends to have a stronger expression in better differentiated and non-metastatic human PDAC tissues. It agrees with the MTA3 expression pattern in endometrioid adenocarcinomas [55] and breast cancer [35]. MTA3-positive carcinomas have a generally good prognosis.

Snail is a core transcriptional factor in mediating EMT, which is also a downstream target of MTA3 in this signaling pathway [35]. E-cadherin, a cell adhesion molecule, is important in anchoring epithelial cells. Changes in Snail and E-cadherin have been proven to correlate with the acquisition of invasiveness in pancreatic cancer [23, 31, 66]. Expression patterns of Snail and E-cadherin in human PDAC tissues were analyzed. Snail and E-cadherin expression was detected in 77% of human PDAC tissues. A higher expression of Snail was observed in poorly differentiated human PDAC tissues than in moderately and moderately to poorly differentiated human PDAC tissues. In contrast, more E-cadherin was associated with a better differentiation of human PDAC tissues (Table 4). These results support the notion that

poor differentiation of pancreatic cancer cell is correlated with EMT [31].

The association between ER α , MTA3, Snail and E-cadherin in human pancreatic cancer tissues was analyzed. Cytoplasmatic ER α staining was found in well differentiated duct-like pancreatic cancer structures, where most of the MTA3, Snail and E-cadherin were also found. In addition, as shown in a series of consecutive sections, a limited number of PDAC cells with nuclear ER α were seen in the duct-like structures with nuclear staining of MTA3, while no Snail was detected in the nucleus in conjunction with strong membrane immunoreactions for E-cadherin (Figure 6). In this study, all human PDAC tissues with positive expression of ER α and MTA3 were in a proliferating status with immunostaining of PCNA in the nucleus (Figure 7).

In clinical samples, ER α , Snail and E-cadherin were detected in human PDAC tissues, and, for the first time, MTA3 was found in human PDAC tissues. These results were comparable to the published findings in breast cancer tissues [35], with ER α and its downstream receptors involved in this EMT-related signaling pathway were observed in the cancer cells. Loss of parts of this signaling pathway (loss of MTA3, expression of Snail, loss of E-cadherin) occurs in a subset of pancreatic cancers, and these pancreatic cancers tend to have a poor clinical differentiation (Table 4). The ER α expression in clinical samples was mostly detected in the cytoplasm, but no correlation was found between cytoplasmatic ER α and nuclear MTA3. A limited number of cancer cells with nuclear ER α were observed, but these cells exhibited a high expression of MTA3, E-cadherin and loss of Snail (Figure 6). This observation was in conflict with the published results that the ER α was mostly located in the nucleus [35, 62]. To further explain this conflict, the localization of ER α was investigated in human pancreatic cancer cell lines.

4.3 Pancreatic cell lines

The pancreatic cancer cell lines provide us with an important tool and experimental model for studying the gene and protein expression patterns, efficacy of therapeutic drugs and biological behavior of pancreatic cancer in vitro. Compared to human samples, where the cancer cells vary drastically even from one patient, cancer cell

lines are alike because they share the same genetic and molecular features from the cancer cell they were derived from. They are also well suited for further experiments and can tell us the differences between different subgroups of cancer cells. To find an appropriate cancer cell line for further interference experiments on this signaling pathway, the expression patterns of ER α and its related factors included in this signaling pathway in pancreatic cancer cells lines were further investigated.

ER α was observed in all pancreatic cancer cell lines with different intensities at the mRNA level, but no signal was detected at the protein level in western-blot (Figure 12, 13). However, compared with MCF-7 cells, immunofluorescence tests disclosed immunoreactions of ER α in the nucleus in all 5 pancreatic cancer cell lines with a weak staining. In the undifferentiated human pancreatic cancer line MiaPaCa-2, about 60% of cancer cells had nuclear ER α staining, followed by PANC-1 and ASPC-1, while the moderately differentiated Capan-1 and HPAF-2 had the weakest expression (Figure 8). This observation supported the fact that ER α is present in pancreatic cancer cells but at a lower level than that seen in breast cancer cells [67]. The differences between expression levels for mRNA and protein of ER α was probably due to the low transcriptional level of ER α in pancreatic cancer cells like in some ER α negative breast cancer cells [68]. Because of the low level of ER α protein, it could only be detected in a more sensitive method such as immunofluorescence staining.

MTA3 was found in all 5 human pancreatic cancer cell lines, with a higher expression in the moderately differentiated human pancreatic cancer cell lines Capan-1 and HPAF-2 at both the mRNA and protein level (Figure 12, 13). Cancer differentiation appeared to be correlated with MTA3 in pancreatic cancer cell lines. Better differentiated cancer cell lines had a tendency to have a higher expression of MTA3. The results obtained from immunocytochemistry tests confirmed the results found in RT-PCR and western blotting (Figure 9). Transcriptional receptor Snail had strong expression in the poorly or undifferentiated cell lines PANC-1 and MiaPaCa-2, but no signal was detected in the moderately differentiated HPAF-2 cell line (Figure 10, 12, 13). In contrast, while strong E-cadherin expression was detected in the Capan-1 and HPAF-2 cell lines, no expression was observed in the undifferentiated MiaPaCa-2 cell

line (Figure 11, 12, 13) [31]. This finding supports the results obtained in human PDAC tissues that Snail is an upstream repressor of E-cadherin. High expression of Snail suppresses E-cadherin and induces EMT, which correlates with poor differentiation in pancreatic cancer cells [31, 66].

Interaction between these factors was found in some pancreatic cancer cell lines. In the moderately differentiated cell line HPAF-2, a strong expression of MTA3 correlated with a weaker Snail expression, followed by a strong expression of downstream E-cadherin (Figure 13). In contrast, in the undifferentiated MiaPaCa-2 cell line, the low MTA3 expression led to a strong expression of Snail with no downstream E-cadherin expression. With decreasing differentiation status, MTA3, Snail and E-cadherin were co-expressed in the pancreatic cancer cell lines. This is in agreement with the hypothesis that in human PDAC cancer lines, MTA3 is an upstream regulator of Snail and E-cadherin that regulates EMT by suppressing Snail and activating E-cadherin [35, 56, 69]. The pancreatic cancer cell lines with loss of MTA3 have a generally poor differentiation and the tendency to grow invasively [35]. Compared with the expression pattern of ER α in human PDAC tissues, the frequency of nuclear localization of ER α in human pancreatic cancer cell lines was higher than that observed in human PDAC tissues. ER α is a ligand-activated transcription factor that regulates gene expression in the nucleus. Upon estrogen binding, ER α transformed and translocated from the cytoplasm to the nucleus and regulated the expression of different genes via binding to specific DNA sequences known as estrogen-responsive elements (ERE) [48]. The results obtained from clinical samples suggested that ER α was present in human pancreatic cancer tissues, but most of it in an inactive form and located in the cytoplasm, since the amount of local estrogen in human PDAC cancer tissues was too low to activate the ER α . With adequate estrogen levels, the activated ER α is able to repress EMT via the ER α /MTA3/Snail/E-cadherin signaling pathway and protect patients from tumor genesis and metastasis [18]. However, in pancreatic cell lines, the media used for cell cultures contain phenol red, which has an estrogen-like activity [70]. The inactivated cytoplasmic ER α was activated by phenol red and translocated into the nucleus. Based on these results, it is

possible that a subset of pancreatic cancer patients with inactivated ER α expression in the cytoplasm as well as MTA3, Snail and E-cadherin, may respond to estrogen therapy. Further experiments are needed to identify the effect of estrogen in human pancreatic cancer cells via this EMT-related signaling pathway. The Capan-1 cell line, with an expression of all of the elements involved in this signaling pathway, would be a suitable candidate for further interference studies.

4.4 Orthotopic xenograft models of pancreatic cells

Orthotopic xenograft models of pancreatic cells, whose human pancreatic tumor originates in the mouse pancreas, resemble the human pancreatic cancer situation in a mouse model. This model is an important tool for gathering information about the changes occurring during tumor progression, like tumor genesis, angiogenesis, lymphangiogenesis and metastasis in a specific subset of pancreatic cancer cells, resembles a specific subset of the human cancer situation and is more equal than human cancer tissues. Since there is no single, perfect model that resembles the human cancer situation, different models would have to be used to study different aspects of a cancer. To strengthen the results obtained from human PDAC tissues and human pancreatic cancer cell lines, ER α and its related elements in human pancreatic cancer cells were investigated in orthotopic nude mice xenografts.

The results obtained from nude mice xenografts were consistent with those observed in *in vitro* experiments. ER α , MTA3, Snail and E-cadherin were found in the pancreatic cancer cells. Low levels of ER α were likewise seen in pancreatic cancer cells. A higher expression of MTA3 tended to be found in better differentiated cells. Moreover, a higher expression of MTA3 was correlated with a lower expression of Snail and a higher expression of E-cadherin. Orthotopic nude mice xenografts of Capan-1 cells expressed all of these elements in this signaling pathway. This indicated that this orthotopic nude mouse xenograft acted as a suitable model for further interventional experiments.

4.5 Conclusion

ER α exists in human pancreatic cancer cells together with MTA3, Snail and E-cadherin, but most of the ER α located in the cytoplasm of human pancreatic cancer cells is found to be inactivated. In a subset of PDAC patients with inactivated cytoplasmatic ER α and MTA3, Snail, E-cadherin, estrogen therapy may be a potential strategy to prevent tumor progression by repressing EMT via the ER α /MTA3/ Snail/ E-cadherin pathway. This agrees with the epidemiological data which indicates that whereas estrogen has a protective effect in reducing the risk of pancreatic cancer in young female patients, the incidence of pancreatic cancer increased with decreasing estrogen levels after the age of 50. The male: female ratio was 2:1 and 1:1 in patients before and after 50 years of age [71]. Thus ER α can be considered a target for the therapeutic modulation of cancer progression in the treatment of pancreatic cancer in patients with this EMT-related signal pathway. In pancreatic cancer cell lines, extra estrogen may activate ER α and lead to changes in downstream elements followed by a change of cell invasiveness via alteration of EMT. It would be interesting to perform further interference experiments to investigate the role played by this ER α -related signal pathway in mediating EMT in human pancreatic cancer cells.

5 References

1. Jemal, A., F. Bray, M.M. Center, et al., *Global cancer statistics*. CA: A Cancer Journal for Clinicians, 2011. **61**(2): p. 69-90.
2. Siegel, R., D. Naishadham, and A. Jemal, *Cancer statistics, 2012*. CA Cancer J Clin, 2012. **62**(1): p. 10-29.
3. Hidalgo, M., *Pancreatic cancer*. N Engl J Med, 2010. **362**(17): p. 1605-17.
4. Moore, M.J., D. Goldstein, J. Hamm, et al., *Erlotinib plus gemcitabine compared with gemcitabine alone in patients with advanced pancreatic cancer: a phase III trial of the National Cancer Institute of Canada Clinical Trials Group*. J Clin Oncol, 2007. **25**(15): p. 1960-6.
5. Buchler, M.W., J. Kleeff, and H. Friess, *Surgical treatment of pancreatic cancer*. J Am Coll Surg, 2007. **205**(4 Suppl): p. S81-6.
6. Cameron, J.L., T.S. Riall, J. Coleman, et al., *One thousand consecutive pancreaticoduodenectomies*. Ann Surg, 2006. **244**(1): p. 10-5.
7. Mallinson, C.N., M.O. Rake, J.B. Cocking, et al., *Chemotherapy in pancreatic cancer: results of a controlled, prospective, randomised, multicentre trial*. Br Med J, 1980. **281**(6255): p. 1589-91.
8. Burris, H.A., 3rd, M.J. Moore, J. Andersen, et al., *Improvements in survival and clinical benefit with gemcitabine as first-line therapy for patients with advanced pancreas cancer: a randomized trial*. J Clin Oncol, 1997. **15**(6): p. 2403-13.
9. Conroy, T., F. Desseigne, M. Ychou, et al., *FOLFIRINOX versus gemcitabine for metastatic pancreatic cancer*. N Engl J Med, 2011. **364**(19): p. 1817-25.
10. Stocken, D.D., M.W. Buchler, C. Dervenis, et al., *Meta-analysis of randomised adjuvant therapy trials for pancreatic cancer*. Br J Cancer, 2005. **92**(8): p. 1372-81.
11. El-Rayes, B.F., M.M. Zalupski, A.F. Shields, et al., *A phase II study of celecoxib, gemcitabine, and cisplatin in advanced pancreatic cancer*. Invest New Drugs, 2005. **23**(6): p. 583-90.
12. Bramhall, S.R., J. Schulz, J. Nemunaitis, et al., *A double-blind placebo-controlled, randomised study comparing gemcitabine and marimastat with gemcitabine and placebo as first line therapy in patients with advanced pancreatic cancer*. Br J Cancer, 2002. **87**(2): p. 161-7.
13. Rocha-Lima, C.M., H.P. Soares, L.E. Racz, et al., *EGFR targeting of solid tumors*. Cancer Control, 2007. **14**(3): p. 295-304.
14. Kalluri, R. and R.A. Weinberg, *The basics of epithelial-mesenchymal transition*. J Clin Invest, 2009. **119**(6): p. 1420-8.
15. Savagner, P., K.M. Yamada, and J.P. Thiery, *The zinc-finger protein slug causes desmosome dissociation, an initial and necessary step for growth factor-induced epithelial-mesenchymal transition*. J Cell Biol, 1997. **137**(6): p. 1403-19.
16. Lochter, A., S. Galosy, J. Muschler, et al., *Matrix metalloproteinase stromelysin-1 triggers a cascade of molecular alterations that leads to stable epithelial-to-mesenchymal conversion and a premalignant phenotype in mammary epithelial cells*. J Cell Biol, 1997. **139**(7): p. 1861-72.
17. Kalluri, R. and E.G. Neilson, *Epithelial-mesenchymal transition and its implications for*

References

- fibrosis*. J Clin Invest, 2003. **112**(12): p. 1776-84.
18. Thiery, J.P., *Epithelial-mesenchymal transitions in tumour progression*. Nat Rev Cancer, 2002. **2**(6): p. 442-54.
 19. Peinado, H., D. Olmeda, and A. Cano, *Snail, Zeb and bHLH factors in tumour progression: an alliance against the epithelial phenotype?* Nat Rev Cancer, 2007. **7**(6): p. 415-28.
 20. Yang, A.D., F. Fan, E.R. Camp, et al., *Chronic oxaliplatin resistance induces epithelial-to-mesenchymal transition in colorectal cancer cell lines*. Clin Cancer Res, 2006. **12**(14 Pt 1): p. 4147-53.
 21. Black, P.C., G.A. Brown, T. Inamoto, et al., *Sensitivity to epidermal growth factor receptor inhibitor requires E-cadherin expression in urothelial carcinoma cells*. Clin Cancer Res, 2008. **14**(5): p. 1478-86.
 22. Frederick, B.A., B.A. Helfrich, C.D. Coldren, et al., *Epithelial to mesenchymal transition predicts gefitinib resistance in cell lines of head and neck squamous cell carcinoma and non-small cell lung carcinoma*. Mol Cancer Ther, 2007. **6**(6): p. 1683-91.
 23. Zhang, K., X. Jiao, X. Liu, et al., *Knockdown of snail sensitizes pancreatic cancer cells to chemotherapeutic agents and irradiation*. Int J Mol Sci, 2010. **11**(12): p. 4891-2.
 24. Tepass, U., K. Truong, D. Godt, et al., *Cadherins in embryonic and neural morphogenesis*. Nat Rev Mol Cell Biol, 2000. **1**(2): p. 91-100.
 25. Yang, J. and R.A. Weinberg, *Epithelial-mesenchymal transition: at the crossroads of development and tumor metastasis*. Dev Cell, 2008. **14**(6): p. 818-29.
 26. Blanco, M.J., G. Moreno-Bueno, D. Sarrio, et al., *Correlation of Snail expression with histological grade and lymph node status in breast carcinomas*. Oncogene, 2002. **21**(20): p. 3241-6.
 27. Bezdekova, M., S. Brychtova, E. Sedlakova, et al., *Analysis of snail-1, e-cadherin and claudin-1 expression in colorectal adenomas and carcinomas*. Int J Mol Sci, 2012. **13**(2): p. 1632-43.
 28. Dohadwala, M., S.C. Yang, J. Luo, et al., *Cyclooxygenase-2-dependent regulation of E-cadherin: prostaglandin E(2) induces transcriptional repressors ZEB1 and snail in non-small cell lung cancer*. Cancer Res, 2006. **66**(10): p. 5338-45.
 29. He, H., W. Chen, X. Wang, et al., *Snail Is an Independent Prognostic Predictor for Progression and Patient Survival of Gastric Cancer*. Cancer Sci, 2012.
 30. Hipp, S., A. Walch, T. Schuster, et al., *Precise measurement of the E-cadherin repressor Snail in formalin-fixed endometrial carcinoma using protein lysate microarrays*. Clin Exp Metastasis, 2008. **25**(6): p. 679-83.
 31. Hotz, B., M. Arndt, S. Dullat, et al., *Epithelial to Mesenchymal Transition: Expression of the Regulators Snail, Slug, and Twist in Pancreatic Cancer*. Clinical Cancer Research, 2007. **13**(16): p. 4769-4776.
 32. Chang, Z.G., J.M. Wei, C.F. Qin, et al., *Suppression of the Epidermal Growth Factor Receptor Inhibits Epithelial-Mesenchymal Transition in Human Pancreatic Cancer PANC-1 Cells*. Dig Dis Sci, 2012.
 33. Rachagani, S., S. Senapati, S. Chakraborty, et al., *Activated KrasG(1)(2)D is associated with invasion and metastasis of pancreatic cancer cells through inhibition of E-cadherin*. Br J Cancer, 2011. **104**(6): p. 1038-48.
 34. Takano, S., F. Kanai, A. Jazag, et al., *Smad4 is essential for down-regulation of E-cadherin*

References

- induced by TGF-beta in pancreatic cancer cell line PANC-1. *J Biochem*, 2007. **141**(3): p. 345-51.
35. Fujita, N., D.L. Jaye, M. Kajita, et al., *MTA3, a Mi-2/NuRD complex subunit, regulates an invasive growth pathway in breast cancer*. *Cell*, 2003. **113**(2): p. 207-19.
36. Leitman, D.C., S. Paruthiyil, O.I. Vivar, et al., *Regulation of specific target genes and biological responses by estrogen receptor subtype agonists*. *Curr Opin Pharmacol*, 2010. **10**(6): p. 629-36.
37. Moutsatsou, P., *The spectrum of phytoestrogens in nature: our knowledge is expanding*. *Hormones (Athens)*, 2007. **6**(3): p. 173-93.
38. Konduri, S. and R.E. Schwarz, *Estrogen Receptor β/α Ratio Predicts Response of Pancreatic Cancer Cells to Estrogens and Phytoestrogens*. *Journal of Surgical Research*, 2007. **140**(1): p. 55-66.
39. Gustafsson, J.A., *Estrogen receptor beta--a new dimension in estrogen mechanism of action*. *J Endocrinol*, 1999. **163**(3): p. 379-83.
40. Zaretsky, J.Z., I. Barnea, Y. Aylon, et al., *MUC1 gene overexpressed in breast cancer: structure and transcriptional activity of the MUC1 promoter and role of estrogen receptor alpha (ERalpha) in regulation of the MUC1 gene expression*. *Mol Cancer*, 2006. **5**: p. 57.
41. Guttilla, I.K., B.D. Adams, and B.A. White, *ERalpha, microRNAs, and the epithelial-mesenchymal transition in breast cancer*. *Trends Endocrinol Metab*, 2012. **23**(2): p. 73-82.
42. Scherbakov, A.M., O.E. Andreeva, V.A. Shatskaya, et al., *The relationships between Snail and estrogen receptor signaling in breast cancer cells*. *J Cell Biochem*, 2012.
43. Zannoni, G.F., M.G. Prisco, V.G. Vellone, et al., *Changes in the expression of oestrogen receptors and E-cadherin as molecular markers of progression from normal epithelium to invasive cancer in elderly patients with vulvar squamous cell carcinoma*. *Histopathology*, 2011. **58**(2): p. 265-75.
44. Park, S.H., L.W. Cheung, A.S. Wong, et al., *Estrogen regulates Snail and Slug in the down-regulation of E-cadherin and induces metastatic potential of ovarian cancer cells through estrogen receptor alpha*. *Mol Endocrinol*, 2008. **22**(9): p. 2085-98.
45. Zhang, Y., P.F. Coogan, J.R. Palmer, et al., *A case-control study of reproductive factors, female hormone use, and risk of pancreatic cancer*. *Cancer Causes Control*, 2010. **21**(3): p. 473-8.
46. Tomao, S., A. Romiti, B. Massidda, et al., *A phase II study of gemcitabine and tamoxifen in advanced pancreatic cancer*. *Anticancer Res*, 2002. **22**(4): p. 2361-4.
47. Eckel, F., C. Lersch, F. Lippl, et al., *Phase II trial of cyclophosphamide, leucovorin, 5-fluorouracil 24-hour infusion and tamoxifen in pancreatic cancer*. *J Exp Clin Cancer Res*, 2000. **19**(3): p. 295-300.
48. Zhang, D. and V.L. Trudeau, *Integration of membrane and nuclear estrogen receptor signaling*. *Comp Biochem Physiol A Mol Integr Physiol*, 2006. **144**(3): p. 306-15.
49. Horwitz, K.B., T.A. Jackson, D.L. Bain, et al., *Nuclear receptor coactivators and corepressors*. *Mol Endocrinol*, 1996. **10**(10): p. 1167-77.
50. Mishra, S.K., A.H. Talukder, A.E. Gururaj, et al., *Upstream determinants of estrogen receptor-alpha regulation of metastatic tumor antigen 3 pathway*. *J Biol Chem*, 2004. **279**(31): p. 32709-15.
51. Kumar, R., R.A. Wang, and R. Bagheri-Yarmand, *Emerging roles of MTA family members in*

References

- human cancers. *Semin Oncol*, 2003. **30**(5 Suppl 16): p. 30-7.
52. Kumar, R., R.A. Wang, A. Mazumdar, et al., *A naturally occurring MTA1 variant sequesters oestrogen receptor-alpha in the cytoplasm*. *Nature*, 2002. **418**(6898): p. 654-7.
53. Lai, A.Y. and P.A. Wade, *Cancer biology and NuRD: a multifaceted chromatin remodelling complex*. *Nature Reviews Cancer*, 2011. **11**(8): p. 588-596.
54. Yu, J.C., H.M. Hsu, S.T. Chen, et al., *Breast cancer risk associated with genotypic polymorphism of the genes involved in the estrogen-receptor-signaling pathway: a multigenic study on cancer susceptibility*. *J Biomed Sci*, 2006. **13**(3): p. 419-32.
55. Bruning, A., J. Juckstock, T. Blankenstein, et al., *The metastasis-associated gene MTA3 is downregulated in advanced endometrioid adenocarcinomas*. *Histol Histopathol*, 2010. **25**(11): p. 1447-56.
56. Jaye, D.L., J. Iqbal, N. Fujita, et al., *The BCL6-associated transcriptional co-repressor, MTA3, is selectively expressed by germinal centre B cells and lymphomas of putative germinal centre derivation*. *J Pathol*, 2007. **213**(1): p. 106-15.
57. Fujita, N., M. Kajita, P. Taysavang, et al., *Hormonal regulation of metastasis-associated protein 3 transcription in breast cancer cells*. *Mol Endocrinol*, 2004. **18**(12): p. 2937-49.
58. Hotz, H.G., H.A. Reber, B. Hotz, et al., *An orthotopic nude mouse model for evaluating pathophysiology and therapy of pancreatic cancer*. *Pancreas*, 2003. **26**(4): p. e89-98.
59. Stierer, M., H. Rosen, R. Weber, et al., *Immunohistochemical and biochemical measurement of estrogen and progesterone receptors in primary breast cancer. Correlation of histopathology and prognostic factors*. *Ann Surg*, 1993. **218**(1): p. 13-21.
60. Kleihues, P. and L.H. Sobin, *World Health Organization classification of tumors*. *Cancer*, 2000. **88**(12): p. 2887.
61. Kreiger, N., J. Lacroix, and M. Sloan, *Hormonal factors and pancreatic cancer in women*. *Ann Epidemiol*, 2001. **11**(8): p. 563-7.
62. Greenway, B., M.J. Iqbal, P.J. Johnson, et al., *Oestrogen receptor proteins in malignant and fetal pancreas*. *Br Med J (Clin Res Ed)*, 1981. **283**(6294): p. 751-3.
63. Singh, S., P.R. Baker, R. Poulson, et al., *Expression of oestrogen receptor and oestrogen-inducible genes in pancreatic cancer*. *Br J Surg*, 1997. **84**(8): p. 1085-9.
64. Yeh, T.S., Y.Y. Jan, C.T. Chiu, et al., *Characterisation of oestrogen receptor, progesterone receptor, trefoil factor 1, and epidermal growth factor and its receptor in pancreatic cystic neoplasms and pancreatic ductal adenocarcinoma*. *Gut*, 2002. **51**(5): p. 712-6.
65. Taylor, O.M., J. Teasdale, P.N. Cowen, et al., *Classical oestrogen receptor is not detectable in pancreatic adenocarcinoma*. *Br J Cancer*, 1992. **66**(3): p. 503-6.
66. von Burstin, J., S. Eser, M.C. Paul, et al., *E-cadherin regulates metastasis of pancreatic cancer in vivo and is suppressed by a SNAIL/HDAC1/HDAC2 repressor complex*. *Gastroenterology*, 2009. **137**(1): p. 361-71, 371 e1-5.
67. Iwao, K., Y. Miyoshi, M. Ooka, et al., *Quantitative analysis of estrogen receptor-alpha and -beta messenger RNA expression in human pancreatic cancers by real-time polymerase chain reaction*. *Cancer Lett*, 2001. **170**(1): p. 91-7.
68. Lambertini, E., L. Penolazzi, S. Magaldi, et al., *Transcription factor decoy against promoter C of estrogen receptor alpha gene induces a functional ER alpha protein in breast cancer cells*. *Breast Cancer Res Treat*, 2005. **92**(2): p. 125-32.
69. Simpson, A., J. Uitto, U. Rodeck, et al., *Differential expression and subcellular distribution of*

References

- the mouse metastasis-associated proteins Mta1 and Mta3*. Gene, 2001. **273**(1): p. 29-39.
70. Berthois, Y., J.A. Katzenellenbogen, and B.S. Katzenellenbogen, *Phenol red in tissue culture media is a weak estrogen: implications concerning the study of estrogen-responsive cells in culture*. Proc Natl Acad Sci U S A, 1986. **83**(8): p. 2496-500.
71. Bourhis, J., F. Lacaine, M. Augusti, et al., *Protective effect of oestrogen in pancreatic cancer*. Lancet, 1987. **2**(8565): p. 977.

Curriculum vitae

Mein Lebenslauf wird aus datenschutzrechtlichen Gründen in der elektronischen Version meiner Arbeit nicht veröffentlicht.

Affidavit

I, Yuhua, Zhang, certify under penalty of perjury by my own signature that I have submitted the thesis on the topic: Expression of estrogen receptor alpha and downstream molecule Metastasis-Associated-Gene 3 (MTA3) in human pancreatic cancer. I wrote this thesis independently and without assistance from third parties, I used no other aids than the listed sources and resources.

All points based literally or in spirit on publications or presentations of other authors are, as such, in proper citations (see "uniform requirements for manuscripts (URM)" the ICMJE www.icmje.org) indicated. The sections on methodology (in particular practical work, laboratory requirements, statistical processing) and results (in particular images, graphics and tables) correspond to the URM (s.o) and are answered by me. My interest in any publications to this dissertation corresponds to those that are specified in the following joint declaration with the responsible person and supervisor. All publications resulting from this thesis and which I am author correspond to the URM (see above) and I am solely responsible.

The importance of this affidavit and the criminal consequences of a false affidavit (section 156,161 of the Criminal Code) are known to me and I understand the rights and responsibilities stated therein.

Date: 10.01.2013

Signature: Yuhua Zhang

Acknowledgements

First of all, I want to thank PD. Dr. Hubert Hotz who supervised the work I present here. I thank Prof. Heinz-Johannes Buhr, for allowing me persuing my MD in General, Visceral and Vascular Surgery Department, Charité Medical University, Berlin, Campus Benjamin Franklin.

First and foremost I thank Mrs. Birgit Hotz, an outstanding technician in our lab, for her kindness, patience and endless efforts not only help me with my research work but also for the critical reading of the manuscript. I thank Marco Arndt for his help of my PCR research. I thank specially Dr Ulrike Erben, for many helpful advices during the laboratory work and critical reading of the manuscript.

I thank Mrs. Pamela Glowacki and Mrs. Zhonghua Helmke from Chaite international cooperation, who paved the way for my life in Berlin. I thank also Jin Du, Juan Luo, Xu Qian, Haitao Wang and Yu Xia who peruse their MDs with me, and with whom I shared most of the good and bad experiences associated to a doctoral thesis.

Lastly, and most importantly, I wish to thank family in China, especially my beautiful wife Xiaoyan Tang and our lovely son, Zitao Zhang. They have always been my constant source of support, and this research work would certainly not have been possible without their unconditional love and encouragement. To my lovely family, I dedicate this doctoral thesis.